HHS Public Access

Author manuscript

Cell Rep. Author manuscript; available in PMC 2022 March 06.

Published in final edited form as:

Cell Rep. 2022 February 15; 38(7): 110363. doi:10.1016/j.celrep.2022.110363.

Redox regulation of age-associated defects in generation and maintenance of T cell self-tolerance and immunity to foreign antigens

Allison K. Hester[1,6], **Manpreet K. Semwal**[1,6], **Sergio Cepeda**[1], **Yangming Xiao**[1], **Meghan Rueda**[1], **Kymberly Wimberly**[1], **Thomas Venables**[2], **Thamotharampillai Dileepan**[3,4], **Ellen Kraig**[5], **Ann V. Griffith**[1,7,*]

[1]Department of Microbiology, Immunology and Molecular Genetics, University of Texas Long School of Medicine, UT Health San Antonio, San Antonio, TX 78229, USA

[2]The Scripps Research Institute, Jupiter, FL 33458, USA

[3]Center for Immunology, University of Minnesota Medical School, Minneapolis, MN 55455, USA

[4]Department of Microbiology, University of Minnesota Medical School, Minneapolis, MN 55455, USA

[5]Department of Cell Systems and Anatomy, University of Texas Long School of Medicine, UT Health San Antonio, San Antonio, TX 78229, USA

[6]These authors contributed equally

[7]Lead contact

SUMMARY

Thymic atrophy reduces naive T cell production and contributes to increased susceptibility to viral infection with age. Expression of tissue-restricted antigen (TRA) genes also declines with age and has been thought to increase autoimmune disease susceptibility. We find that diminished expression of a model TRA gene in aged thymic stromal cells correlates with impaired clonal deletion of cognate T cells recognizing an autoantigen involved in atherosclerosis. Clonal deletion in the polyclonal thymocyte population is also perturbed. Distinct age-associated defects in the generation of antigen-specific T cells include a conspicuous decline in generation of T cells recognizing an immunodominant influenza epitope. Increased catalase activity delays thymic atrophy, and here, we show that it mitigates declining production of influenza-specific T cells and

*Correspondence: griffitha3@uthscsa.edu.

AUTHOR CONTRIBUTIONS

Conceptualization, A.V.G., A.K.H., and M.K.S.; investigations, A.K.H., M.K.S., S.C., Y.X., M.R., K.W., and T.V.; formal analysis, A.K.H., M.K.S., S.C., Y.X., M.R., T.V., and A.V.G.; resources, T.D. and T.V.; writing – original draft, A.V.G. and E.K.; writing – review & editing, A.K.H., M.K.S., S.C., Y.X., M.R., K.W., T.V., T.D., E.K., and A.V.G.; funding acquisition and supervision, E.K. and A.V.G.

DECLARATION OF INTERESTS

The authors declare no competing interests.

SUPPLEMENTAL INFORMATION

Supplemental information can be found online at https://doi.org/10.1016/j.celrep.2022.110363.

their frequency in lung after infection, but does not reverse declines in TRA expression or efficient negative selection. These results reveal important considerations for strategies to restore thymic function.

In brief

Age-associated thymic dysfunctions increase susceptibility to infection by diminishing T cell generation and may also impair T cell tolerance. Hester et al. demonstrate age-associated declines in tolerance induction, including impaired tolerance to an atherosclerosis autoantigen. Catalase overexpression delays thymic atrophy and mitigates declines in influenza-specific T cells, but does not rescue impaired central tolerance.

Graphical Abstract

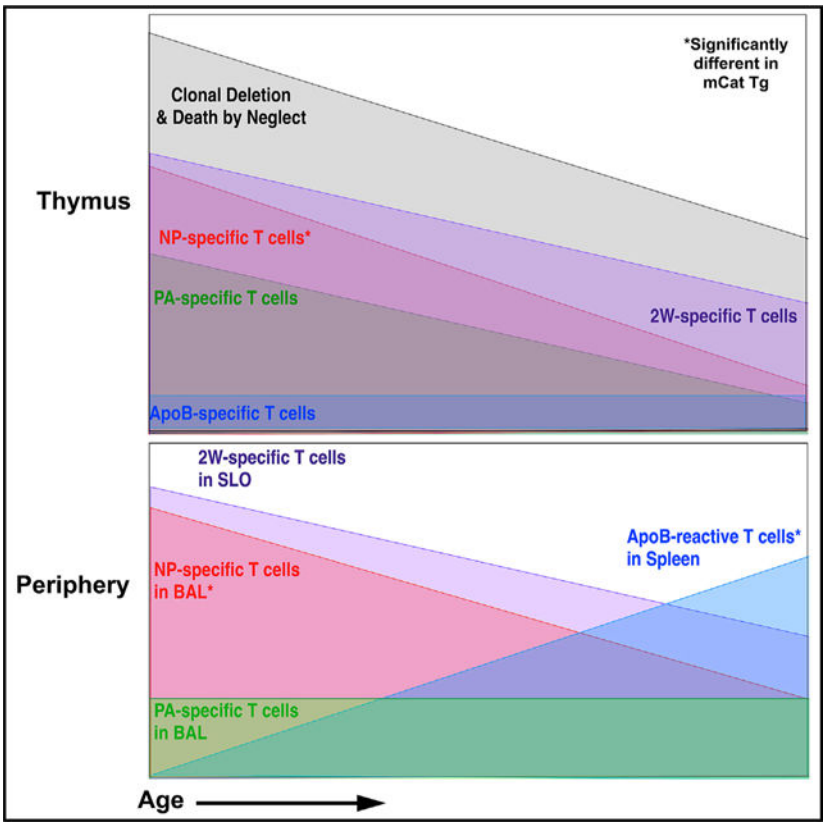

INTRODUCTION

The thymus is the primary site of T cell maturation. Production of new naive T cells depends on the availability of lymphopoietic niches within the thymic microenvironment (Bhandoola et al., 2007; Prockop and Petrie, 2004), to which circulating multi-potent progenitors are periodically recruited (Foss et al., 2001; Goldschneider et al., 1986; Luc et al., 2012; Luis et al., 2016). However, the size of the thymus begins to decline relatively early in life, concomitant with diminished production of T cells (Aspinall et al., 2010; Hale et al., 2006; Hartwig and Steinmann, 1994; Steinmann et al., 1985). Compensatory

peripheral homeostatic expansion and continued antigenic experience result in a shift toward an oligoclonal memory T cell population with declining T cell receptor (TCR) diversity (Ahmed et al., 2009; Britanova et al., 2014; Callahan et al., 1993; Ernst et al., 1990; Hale et al., 2006; Haynes et al., 2000; Nikolich-Zugich and Rudd, 2010; Posnett et al., 1994; Sempowski et al., 2002; Smithey et al., 2012; Utsuyama et al., 1992; Yoshida et al., 2017). Immunological sequelae include diminished responsiveness to vaccines and tumor surveillance and decreased responsiveness to novel pathogens (Brien et al., 2009; Gil et al., 2015; Lee et al., 2011; Palmer et al., 2018; Stacy et al., 2003).

Paradoxically, aging is also associated with increases in circulating autoantibodies as well as increased susceptibility to some autoimmune disorders (reviewed in Cooper and Stroehla, 2003 and Goronzy and Weyand, 2012); the underlying mechanisms regulating this increase are not completely understood. Age-associated thymic atrophy has been considered a likely contributor to declines in central T cell tolerance induction (e.g., Muller and Pawelec, 2015), and several studies have demonstrated age-associated decreases in thymic function in addition to loss of mass (Baran-Gale et al., 2020; Ki et al., 2014). Diminished expression of tissue-restricted antigen (TRA) genes in thymic antigen-presenting cells, which is critical for tolerizing developing T cells, has also been reported in mice and humans (Baran-Gale et al., 2020; Bredenkamp et al., 2014; Cepeda et al., 2018; Derbinski et al., 2005; Gies et al., 2017; Griffith et al., 2012; Klein et al., 2014). There is also relatively new evidence to support the notion that thymus atrophy is associated with declines in negative selection of autoreactive T cells with age and in a mouse model of thymus atrophy induced by *Foxn1* deficiency (Baran-Gale et al., 2020; Coder et al., 2015).

These studies reveal a potential mechanistic link between age-associated autoimmunity and thymic dysfunction. Declining TRA expression in thymic antigen-presenting cells (APCs) could reasonably be expected to result in diminished negative selection of potentially autoreactive T cells, but little direct evidence for this hypothesis exists. It is also possible that the declines in TRA expression are not of sufficient magnitude to affect T cell selection and/or that increased generation of self-reactive T cells in the thymus could be entirely compensated for by thymic atrophy, such that “escape” of self-specific T cells from the thymus would still decline. Diminished negative selection could also be compensated for by thymic or peripheral diversion to the regulatory T cell lineage. Studies focused on these questions have been hampered by the paucity of T cells recognizing any particular self-antigen (approximately 20–200 T cell total per mouse; Moon et al., 2007). Here, we take complementary approaches to overcome this technical barrier.

RESULTS

Aging is associated with defective negative selection of polyclonal T cells, which is not rescued by delayed thymic atrophy in mCat Tg mice

To assess the impact of aging on thymic selection, we employed a recently reported flow cytometric approach to measure clonal deletion in the polyclonal T cell population based on identification of cleaved caspase 3 among signaled ($TCR^{hi}CD5^{hi}$) thymic T cells (after exclusion of cells expressing CD25, NK1.1, and TCRγ/δ; Figure 1A; Breed et al., 2019). Although the frequencies of $CD4^{+}CD8^{+}$ double-positive (DP) lymphocytes that had been

signaled and were available for positive selection were similar in 6-month-old wild-type (WT) mice relative to 5-week-old WT animals (Figure 1B), we found that the expression of CD5 within that signaled population was diminished in the older mice (Figure 1C). Moreover, within the DP "signaled" population, the frequency of cells undergoing clonal deletion was decreased (Figure 1E). The total number of cells in each group declined, as expected given the significant thymic atrophy that has occurred at this age (Figure S1). We likewise found decreased clonal deletion among SP4 and SP8 T cells (Figures 1F and 1G). Among non-signaled cells, we found a decrease in the frequency of cells undergoing death by neglect in the older mice (Figure 1D). Together, these studies suggest that the efficiency of clonal deletion of self-specific T cells declines with age, concomitant with diminished TCR signaling as indicated by CD5 expression. These data are in agreement with recent work indicating decreased negative selection in aged mice among single-positive (SP) cells (Baran-Gale et al., 2020), also assessed using a different flow cytometric approach (Hu et al., 2016). In that study, decreases in negative selection at earlier (double-negative [DN]/ double-positive [DP]) stages were not found. This discrepancy could be due to differences in the flow cytometric approaches. These results also suggest defects in positive selection occur in aging, which are presumably independent of changes in TRA expression, since non-signaled cells appear to undergo death by neglect at a lower frequency in older mice.

We next investigated whether these changes in selection were rescued in mice in which thymic atrophy was mitigated by transgenic overexpression of catalase (Schriner et al., 2005). Previously, we showed that thymic atrophy results in large part from oxidative damage in stromal cells caused by a deficiency in the expression of the hydrogen peroxide quenching enzyme catalase in this population. Complementation of this deficiency, accomplished by overexpression of a mitochondrially targeted catalase transgene (mCat Tg), resulted in an increase in the size of the thymus by about 2-fold in 6-month-old mCat Tg mice relative to WT controls (Griffith et al., 2015). In contrast to the effect on thymus size, none of the age-associated perturbations in selection were rescued in age-matched mCat Tg mice (Figures 1B–1D). Thus, the age effects on clonal deletion, and possibly on positive selection, are not prevented when thymic atrophy is delayed by reducing oxidative damage.

Effects of age and delayed thymic atrophy on negative selection of $ApoB_{P6}$-specific T cells

As an initial step toward directly addressing the impact of age-associated declines in thymic TRA gene expression on negative selection, we focused on T cells recognizing a model TRA encoded by the apolipoprotein B (ApoB) gene. We previously identified apolipoprotein B as a TRA expressed in medullary stromal cells using a bioinformatic approach (Griffith et al., 2012). Like many TRAs (Griffith et al., 2012), the levels of ApoB RNA decline with age in the thymic medulla (Figure 2A). Studies have shown that $ApoB_{978–993}$, referred to herein as $ApoB_{P6}$, functions as an autoantigen implicated in atherosclerosis in mice and humans (Hermansson et al., 2010; Shaw et al., 2017; Tse et al., 2013). In a mouse model of atherosclerosis (Apoe knockout mice [$Apoe^{-/-}$]; Lo Sasso et al., 2016), interferon (IFN)-γ-producing CD4 T cells accumulate in the arterial walls, promoting atherosclerosis by increasing inflammation and foam cell formation (Hermansson et al., 2010; Koltsova et al., 2012). ApoBp:I-A^b tetramers have been used to show that ApoB-responsive T cells accumulate in aortic plaques and exacerbate atherosclerosis in the $Apoe^{-/-}$ model (Shaw et

al., 2017). In similar mouse models prone to atherosclerosis, regulatory T cells recognizing the same epitope, $ApoB_{P6}$, are capable of ameliorating disease severity (Kimura et al., 2015, 2017, 2018); this highlights the importance of the balance between generation of conventional T cells (T_{conv} cells) and regulatory T cells (T_{reg} cells) recognizing $ApoB_{P6}$.

Using $ApoB_{P6}$:I-A^b major histocompatibility complex class II (MHC class II) tetramers (a generous gift from Dr. Marc Jenkins), we measured T cells specific for $ApoB_{P6}$ in the thymus of young (5-week-old) and older (6-month-old) mice (Figures 2B and 2D). By 6 months of age, the thymus has already deteriorated significantly, having lost approximately 75% of its cellularity relative to its peak size in 5-week-old mice (Dominguez-Gerpe and Rey-Mendez, 2003; Griffith et al., 2015). Thus, barring changes in selection efficiency, the total number of T cells recognizing any given antigen would likewise be expected to decline by about 75%. When we measured the total number of T cells recognizing a representative foreign antigen, a variant of peptide 52–68 of the I-Eα chain (Dongre et al., 2001), using an MHC class II tetramer, designated 2W:I-A^b (also a gift from Dr. Marc Jenkins), we found that the total number of T cells recognizing 2W was indeed decreased significantly (>2-fold) in 6-month-old mice relative to mice at 5 weeks of age (Figure 2C). In contrast, the number of T cells recognizing the $ApoB_{P6}$ self-antigen did not change at 6 months of age (Figure 2D). These results are consistent with the notion that the levels of $ApoB_{P6}$-specific T cells generated in the aged thymus are maintained in older animals due to a loss of negative selection and a consequent failure of clonal deletion with aging.

However, the $ApoB_{P6}$-specific T cells detected may represent either potentially autoreactive T_{conv} cells or tolerizing T_{reg} cells, as both would have been enumerated as tetramer-binding cells. Thus, we next used intracellular Foxp3 staining in combination with tetramer staining to identify $ApoB_{P6}$-specific T_{reg} cells but found that the small number of tetramer-binding T cells recovered from the aged thymus precluded accurate estimation of the frequency of $FoxP3^+$ cells within this population (Figure S2). As a result, we assessed the effects of aging on T_{reg} cells in the periphery, where greater numbers of antigen-specific T cells could be analyzed (Figure 4).

Since we had previously found that complementation of catalase activity in mice overexpressing a mCat Tg resulted in delayed thymic atrophy (Griffith et al., 2015), we investigated whether the selection of $ApoB_{P6}$-specific T cells in the older mice was rescued when thymus atrophy was delayed in 6-month-old mCat Tg mice. As shown in Figure 2D, the total number of $ApoB_{P6}$-specific T cells increased significantly in 6-month-old mCat Tg mice relative to age-matched WT animals, consistent with the overall increase in total thymocyte number in mCat Tg mice (Griffith et al., 2015). The number of 2W-specific T cells also trended higher in aged mCat Tg mice relative to WT, but this difference was not statistically significant. Since negative selection of $ApoB_{P6}$-specific T cells was not rescued in mCat Tg mice, we next asked whether expression of ApoB and other TRAs was increased in aged mCat Tg mice relative to age-matched WT mice. Previously published gene expression data measured by microarray from microdissected whole medullary tissue in 12-month-old WT mice (GSE132136; n = 3) were compared with samples microdissected from 12-month-old mCat Tg mice (n = 3) mice as previously described (Griffith et al., 2009, 2012; Venables et al., 2019). Using our previously generated TRA list, we found that the

age-associated decline in TRA expression in general, and expression of ApoB in particular (shown in red), was not rescued in aged mCat Tg mice (Figure 3A). A list of genes that were differentially expressed is included in Table S1. This was consistent with global gene expression, which was also not fully rescued, as indicated by segregated hierarchical clustering among the aged WT and mCat Tg thymic medulla relative to young medulla (Figure 3B). These results suggest that the larger thymus in aged mCat Tg mice, similar to the regenerated thymus induced by castration (Griffith et al., 2012), does not retain a young transcriptome and may not retain healthy function similar to young mice, at least in terms of appropriate T cell repertoire selection.

Tolerance to $ApoB_{P6}$ declines in the periphery of aged mice and is rescued by catalase overexpression

To investigate the potential for autoreactivity among $ApoB_{P6}$-specific T cells that leave the thymus and seed the periphery, we next measured the total number of antigen-specific T cells in the secondary lymphoid organs (SLOs) (spleen and lymph nodes). We found that, while there was a decrease in the number of 2W-specific T cells with age in WT mice, there was a significant increase in the number of $ApoB_{P6}$-specific T cells in 6-month-old WT mice relative to 5-week-old mice (Figures 4A and 4C), consistent with continued output of ApoB $_{P6}$-specific T cells from the thymus of aged mice. However, the number of 2W- and $ApoB_{P6}$-specific T cells in 6-month-old mCat Tg SLOs was similar to age-matched WT mice (Figures 4A and 4C), although the number of 2W-specific T cells trended higher and the number of $ApoB_{P6}$-specific T cells trended lower in aged mCat Tg mice relative to age-matched WT. We found that the frequency of T_{reg} cells among $ApoB_{P6}$-specific T cells was not significantly changed with age in WT mice; however, there was a significant increase in T_{reg} cell frequency among $ApoB_{P6}$-specific T cells in 6-month-old mCat Tg SLOs relative to age-matched WT mice (Figure 4D). There were no significant differences in $FoxP3^+$ frequency among 2W-specific T cells, although the frequencies trended in the same directions as in the $ApoB_{P6}$-specific T cells (Figure 4B). Nevertheless, the frequencies of T_{conv} and T_{reg} cells may or may not directly correspond to functional responsiveness to antigen encounter.

To determine the effect of these changes in T_{conv} cell/T_{reg} cell balance on the functional responses to the $ApoB_{P6}$ self-antigen, we immunized mice with the $ApoB_{P6}$ peptide in complete Freund's adjuvant (CFA). After 2 weeks, we measured the splenic $CD4^+$ T cell responses to $ApoB_{P6}$ by IFN-γ enzyme-linked immune absorbent spot (ELISpot). We found a significant, approximately 3-fold increase in the frequency of $ApoB_{P6}$-responsive T cells in 12-month-old mice relative to 5-week-old mice (Figure 4D). Remarkably, this increase was entirely mitigated in 12-month-old mCat Tg mice. These data suggest that the increased frequency of T_{reg} cells among peripheral $ApoB_{P6}$-specific T cells in mCat Tg mice results in functional tolerance to the self-antigen; however, given the lack of phenotypic rescue in the thymus of aged mCat Tg mice, it was unclear whether this difference was a result of changes conferred in the thymus or periphery.

To further investigate the phenotype of the $ApoB_{P6}$-specific T cells in aged mice, we measured the expression of several genes in individual $ApoB_{P6}$-specific T cells using

qRT-PCR with the Fluidigm Biomark system. We sorted ApoBp:I-A^b tetramer$^+$ T cells from the SLOs of three young WT mice (28 cells), four aged (12- to 18-month-old) WT mice (37 cells), and five aged mCat Tg mice (36 cells). Despite the large increase in $ApoB_{P6}$-responsive T cells found by ELISpot in aged mice (4e), we found relatively little change in phenotype in $ApoB_{P6}$-specific T cells from aged WT mice relative to young. We found similar expression of CD44, Helios, and Ki67 in ApoB-specific T cells in older mice relative to young (Figures 4F and 4G), with a relatively even mix of CD44$^-$ and CD44$^+$ cells and with most cells expressing both Ki67 and Helios. The expression of T_{reg}-cell- and anergy-associated genes, including FoxP3, FR4 (Yamaguchi et al., 2007), and CD73 (Kalekar and Mueller, 2017), were also similar in young and aged WT mice. These data suggest that the relative contribution of peripheral expansion versus new T cells emigrating from the thymus is similar in young and aged mice. This is consistent with the fact that the total number of $ApoB_{P6}$-specific T cells produced in the aged thymus is similar to young, despite the overall smaller size of the aged thymus. This suggests that the diminished negative selection occurring in the aged thymus contributes to the increased number of $ApoB_{P6}$-specific T cells in the periphery of aged mice. One notable difference between young and aged ApoB-specific T cells was an increase in the frequency of IFN-γ^+ cells with age, consistent with the increased IFN-γ-producing cells among this population revealed by ELISpot.

The observation that some FoxP3$^+$ $ApoB_{P6}$-specific T cells expressed IFN-γ (Figures 4F–4H) is consistent with a recent study demonstrating populations of $ApoB_{P6}$-specific T cells expressing a mixed T_{reg} cell/$T_{effector}$ cell phenotype in both Apoe$^{-/-}$ atherosclerosis-prone mice and in atherosclerosis patients (Wolf et al., 2020), which accumulate prior to onset of disease and exacerbate disease in adoptive transfer experiments. Our results suggest that accumulation of these cells begins relatively early in life and that dysregulated central tolerance induction to $ApoB_{P6}$ in the aged thymus may contribute to their accumulation.

Consistent with our flow cytometry results, our single-cell qRT-PCR analysis also suggested modest increases in the frequency of FoxP3$^+$ cells among ApoB-specific T cells in aged mCat Tg mice relative to WT; however, the frequency of IFN-γ expression among these cells appeared to be even higher than in aged WT ApoB-specific T cells (Figures 4F–4H). The aged mCat Tg ApoB-specific T cells also appeared to express higher levels of CD44 and Ki67 relative to aged WT cells and lower Helios levels relative to WT, suggesting that greater peripheral expansion occurs in aged mCat Tg relative to WT. The increased total number of ApoB-specific T cells in the aged mCat Tg thymus relative to WT suggests that the output of greater numbers of potentially autoreactive T cells in the aged mCat thymus is compensated for in the periphery in order to allow expansion of T cells that are functionally regulatory or quiescent rather than autoreactive. The most striking difference between peripheral ApoB-specific T cells in aged WT and aged mCat Tg mice was an increase in expression of FR4 (Figures 4F and 4G), together with high levels of CD73. These data indicate that the peripheral environment in aged mCat Tg mice promotes anergy induction in what may otherwise be potentially pathogenic “mixed” phenotype T_{reg}/T_{h1} cells. Liver is the tissue with maximal ApoB expression (bioGPS.org); however, we found no significant differences in ApoB expression in mCat Tg mice (Figure S3). Further work will be required to uncover the relative contributions of thymic versus peripheral changes in

aged mCat Tg mice to tolerance in the aged ApoB-specific T cell population, as well the molecular mechanisms regulating that tolerance.

Loss of influenza-specific T cell response emerges by 6 months of age and is rescued by dietary and genetic complementation of stromal catalase deficiency

Paradoxically, aging is associated not only with loss of self-tolerance but also with loss of naive T cell responsiveness to novel antigens and pathogens (Haynes et al., 2003; Sanchez et al., 2001; Stacy et al., 2003), especially viral pathogens (reviewed in Nikolich-Zugich and Rudd, 2010). A well-characterized example is the "hole" in the aged CD8 T cell repertoire recognizing the influenza epitope designated $NP_{366–374}/D^b$ (NP). Previous work by Yager et al. (2008) showed that, at 18 months of age, T cells recognizing the NP, but not $PA_{224–233}/D^b$ (PA) immunodominant influenza epitope, were significantly decreased in the bronchial alveolar lavage (BAL) in mice 10 days after infection with influenza virus.

Given the delayed thymic atrophy in mCat Tg mice, we next investigated whether the larger thymus in aging mCat Tg mice affected NP- and PA-specific T cell responses to influenza. We infected 5-week-old and 6-month-old mice with influenza virus intranasally and assessed influenza-specific T cells frequency in BAL 10 days later. Using NP- and PA-specific MHC class I tetramers (generous gifts from Dr. Blackman and the Molecular Biology Core Facility [MBCF] at Trudeau Institute), we first tested whether declines in flu-specific T cells were apparent by 6 months of age in WT mice. Although the numbers of PA-specific T cells were maintained at 6 months of age (Figures 5A and 5C), as reported for 18-month-old mice (Yager et al., 2008), NP-specific T cells (Figures 5A and 5B) were significantly decreased by approximately 3-fold in the 6-month-old mice. The decline in NP-specific T cell frequency was rescued by the expression of the catalase transgene (Figure 5B). To investigate whether a similar rescue of NP-specific T cell frequency was achieved by dietary antioxidant supplementation, we treated WT mice with water supplemented with the n-acetylcysteine (NAC) beginning at weaning. Our previous work showed that this treatment delayed thymic atrophy at 10 weeks of age in WT mice (Griffith et al., 2015), but we found that the delay in thymic atrophy was not maintained at 6 months of age (Figure 5D). Despite the loss of impact on thymus size between 10 weeks and 6 months of age, we found that 6-month-old NAC-treated mice, like mCat Tg mice, maintained an NP-specific T cell response in BAL similar to that found in young WT mice (Figure 5B).

To evaluate the generation of flu-specific T cells in the thymus, we measured NP- and PA-specific T cells in naive thymi from 5-week-old WT, 14-week-old WT, and 14-week-old mCat Tg mice (Figure 5E). Although 14-week-old mice are not aged, the thymus is significantly atrophied at this time, having lost about half of its peak cellularity or more, and our previous work indicated that atrophy is significantly delayed in mCat Tg mice at this age (Griffith et al., 2015). We found that both NP- and PA-specific T cells were significantly diminished in the thymus 14-week-old mice relative to those at 5 weeks of age. Notably, the age-associated decline in PA-specific T cells appeared to be roughly proportional to the overall decline in thymus cellularity at 14 weeks (decreased by about 50%), similar to what we found for the decline in 2W-specific T cells in the 6-month-old thymus (where thymus size is decreased by about 60%; Figure 2), whereas the NP-specific T cells declined even

more significantly than overall thymus cellularity, by about 70%. NP-specific T cell numbers were significantly higher in thymi from 14-week-old mCat Tg mice relative to age-matched controls, while PA-specific T cell numbers did not significantly increase in mCat Tg mice. We were not able to recover significant numbers of tetramer$^+$ cells in BAL from aged naive mice for comparison. These data suggest that, while production of T cells recognizing foreign antigens generally decreases with age, this effect is not uniform and may be more profound for some T cell specificities relative to others.

Similarly, the effect of catalase overexpression on age-associated changes in generation of T cells recognizing foreign antigens is not uniform. The number of NP-specific T cells produced in mCat Tg thymi during atrophy is increased relative to age-matched controls (Figure 5E), which is consistent with an increase in precursor frequency in aged mCat Tg mice. Changes in the periphery of aged mCat Tg mice may also contribute to the increase in NP-specific T cells in the BAL of aged mice after infection. In contrast, the number of PA-specific T cells in the mCat Tg thymi is similar in 14-week-old mCat Tg and control thymi (Figure 5E). The number of 2W-specific T cells trended higher in mCat Tg thymi relative to controls (Figure 2), but the difference was not statistically significant. Together, these results suggest that catalase overexpression may differentially affect selection of T cells depending on their TCR specificity. Differential effects of catalase overexpression are also seen in young mice, where the number of PA-specific, but not NP-specific, T cells is increased in mCat Tg mice relative to controls (Figure 5E).

DISCUSSION

The narrowing of the naive T cell repertoire that results from thymic atrophy restricts the magnitude of the T cell response to new infections by reducing the number of naive T cells capable of mounting a robust response against a given antigen (reviewed in Nikolich-Zugich and Rudd, 2010). However, the thymus retains a remarkable capacity to regenerate after removal of a negative stimulus (Sutherland et al., 2005) or provision of a positive stimulus (Chaudhry et al., 2016; Chu et al., 2008; Dudakov et al., 2012; Majumdar and Nandi, 2017; Montecino-Rodriguez et al., 1998; Rode and Boehm, 2012; Rossi et al., 2007), but age progressively limits the size reached at return to steady state (reviewed in Cepeda and Griffith, 2018). Nonetheless, even transient regeneration has positive impacts on immunity to microbial infections and tumor surveillance (Heng et al., 2012), and engineering novel approaches to increase thymic activity represents an active area of research (e.g., Bredenkamp et al., 2015; Dudakov et al., 2012; Fahy et al., 2019; Garfin et al., 2013; Hun et al., 2017; Kim et al., 2015; Parent et al., 2013; Shah et al., 2019; Shukla et al., 2017; Sun et al., 2013). A limited understanding of the underlying causes of thymic atrophy has hampered progress toward reversing or delaying its progression. It is clear, however, that atrophy is primarily driven by changes in stromal cells (recently reviewed in Lepletier et al., 2015 and Masters et al., 2017). We recently identified a deficiency in the peroxide-quenching enzyme catalase in thymic stromal cells that results in accumulation of reactive oxygen species (ROS)-induced DNA damage, which is found at much higher levels in TECs relative to lymphocytes in the thymus. This oxidative damage promotes thymic atrophy, which is mitigated by dietary or genetic complementation of antioxidant activity (Griffith et al., 2015). Since the magnitude of the effector T cell response to a

given novel antigen is correlated with the size of the related naive T cell pool (Nelson et al., 2015), delayed thymic atrophy would in turn be predicted to increase the breadth of antigens to which T cells could respond. The increase in NP-specific T cells in thymus of 14-week-old mCat Tg mice relative to age-matched WT mice and the corresponding increase in NP-specific T cells in the BAL of 6-month-old mCat Tg mice relative to age-matched WT mice after influenza infection suggest that this is the case. Remarkably, the increase in NP-specific T cells in BAL was also found in NAC-treated mice, despite the fact that the impact of NAC on thymus size did not persist at 6 months of age (Figure 5).

However, it is notable that the age-associated declines in generation of T cells recognizing two other foreign antigens, PA- and 2W-specific T cells, were not significantly rescued in mCat Tg thymi (although the 2W-specific T cell number trended higher), suggesting that, beyond impacts on overall thymus size, decreased oxidative stress may impact T cell selection differentially, depending on T cell specificity. Consistent with this notion, production of T cells with some specificities (for instance, PA) was significantly different in young mCat Tg relative to controls (Figure 5). Together, these results suggest that both aging and the redox status of stromal cells have independent and variable effects on T cell generation and maintenance, depending on the antigen specificity of the T cell.

In the periphery, we find that the phenotype of $ApoB_{P6}$-specific T cells from aged mice resemble those in young mice, with similar expression of CD44, Ki67, and Helios, consistent with continued output of $ApoB_{P6}$-specific T cells in the aged thymus, despite substantial atrophy. These studies are consistent with the hypothesis that diminished expression of ApoB in the aged thymic medulla results in defective induction of central tolerance to $ApoB_{P6}$ (Figure 2) and a corresponding increase in $ApoB_{P6}$-responsive T cells in the periphery with age (Figure 4), suggesting that, in addition to increased exposure to the autoantigen in susceptible mice, age-associated declines in central T cell tolerance induction may contribute to accumulation of potentially pathogenic $ApoB_{P6}$-specific T cells. One potential alternative explanation may be provided by recent work indicating that self-specific $Foxp3^{-}$ $CD4^{+}$ T cells may be directed to an anergic state in the thymus, in addition to being deleted or diverted to the T_{reg} cell lineage (Hassler et al., 2019). It may be that $Foxp3^{-}$ $ApoB_{P6}$-specific T cells generated in the thymus of young mice tend to be anergic, while those generated in older mice have more effector potential. Recent work has also demonstrated increased persistence of naive T cells generated at later stages of the lifespan (Reynaldi et al., 2019), indicating that potentially dysfunctional naive T cells produced in the aged thymus may tend to outcompete those generated in the young thymus over time.

Limitations of the study

These tetramer studies, together with the decline in clonal deletion in the physiological, polyclonal intrathymic T cell population (Figure 1), provide direct support for the hypotheses that the efficiency of T cell tolerance induction in the thymus declines with age and that age-associated declines in TRA expression contribute to increased T cell autoreactivity. The decrease in frequency of cells undergoing clonal deletion in older mice may reflect a higher frequency of self-specific T cells being positively selected into the T_{conv} cell pool. Alternatively, this decrease in the frequency of cells undergoing clonal deletion

may also result from an increase in diversion to the T_{reg} cell lineage among cells that would have otherwise undergone negative selection. Further work will be required to assess the impact of these changes on the full spectrum of T cell repertoire selection, as well as to comprehensively address the causes for alterations in T cell selection with age.

The balance of evidence suggests that, at early stages of aging, at least up to 12 months of age in mice, stromal cells, rather than lymphocytes, are the primary targets of age-associated dysfunction in the thymus, although a broad spectrum of age-associated changes in hematopoietic cells certainly have profound consequences for immunity later in life (Montecino-Rodriguez et al., 2013). Therefore, although we have not ruled out the possibility that T-cell-intrinsic changes occur, we propose that the age-associated defects in selection reported here primarily represent dysfunctions in stromal cells rather than T-cell-intrinsic deficiencies. Because our previous work showed that expression of the mCat transgene in thymic stromal cells was necessary and sufficient for mitigation of thymic atrophy (Griffith et al., 2015), it is likewise likely that the increased numbers of NP-specific T cell in the aged mCat Tg thymus arise primarily due to the increase in total thymus size mediated by reduced oxidative damage to thymic stromal cells, though our studies do not rule out T-cell-intrinsic effects of catalase overexpression. Together, these studies suggest that preventing or delaying thymic atrophy by reducing oxidative damage in thymic stromal cells may enhance the breadth of microbial antigens recognized by T cells; however, further studies will be required to reveal the mechanisms regulating declining TRA expression in the aged thymus, as well as the mechanisms governing redox regulation of selection in the thymus, and autoreactivity in peripheral T cells.

STAR★METHODS

RESOURCE AVAILABILITY

Lead contact—Further information and requests for resources and reagents should be directed to and will be fulfilled by the lead contact, Ann V. Griffith, PhD (griffitha3@uthscsa.edu).

Materials availability—This study did not generate new unique reagents.

Data and code availability—Microarray data have been deposited at GEO and are publicly available as of the date of publication. Accession numbers are listed in the key resources table.

Any additional information required to reanalyze the data reported in this paper is available from the lead contact upon request. All data reported in this paper will be shared by the lead contact upon request.

This paper does not report original code.

EXPERIMENTAL MODEL AND SUBJECT DETAILS

Mice—C57BL/6J mice (JAX: 000664) and mCAT Tg mice (Schriner et al., 2005; Jax: 016197) were purchased from The Jackson Laboratory (Bar Harbor, ME, USA) at 4–6

weeks of age. All mice used in the experiments were bred and maintained at The University of Texas Health Science Center at San Antonio animal facility under specific pathogen free conditions. Male and female mice were aged and experiments were performed at the indicated ages. No differences in males and females were found and therefore sexes were pooled. For antioxidant supplementation experiments, C57BL/6J male and female mice were weaned at 3 weeks and placed immediately on water supplemented with N-acetyl-L-cysteine (NAC) (15 mg/mL) (Sigma-Aldrich) and allowed to drink *ad libitum*. Water was changed twice weekly until euthanasia. All studies were approved by the Institutional Animal Care and Use Committee.

METHOD DETAILS

Body and thymus weights of NAC-treated mice—Upon euthanasia, mouse body weight was recorded. The thymus was then removed and placed immediately into ice-cold FACS buffer (HBSS, 5% FBS, 0.5% DNAse (1 mg/mL), pH 7.2). To weigh the thymus, the thymus was briefly blotted to remove excess buffer and weight recorded.

ApoB tetramer-based enrichment and staining—Tetramer-binding cells were enriched as described (Moon et al., 2007, 2009). Briefly, a single cell suspension was prepared from thymus, or spleen and lymph nodes (secondary lymphoid organs, SLO) in RPMI 1640c medium with 10% FBS and 2% 1M HEPES buffer. Cells were washed twice in HBSS with 10% FBS. Cells were incubated in 50 nM Dasatinib (Tocris Bioscience) for 30 minutes at 37°C. CD16/CD32 mouse BD Fc-Block (Clone: 2.4G2) along with 2W:I-A^b PE- and APC- labeled tetramers, or $ApoB_{P6}$:I-A^b PE- and APC- labeled tetramers, were added directly to Dasatinib-treated cells at a working concentration of 10 nM. Cells were then incubated in the dark at room temperature for 1 hour followed by washing in 8 mL of ice-cold FACS sorting buffer (FACs buffer with 0.1% sodium azide). Tetramer stained cells were resuspended in a volume of 0.13 mL of sorter buffer and mixed with 0.025 mL of anti-PE and anti-APC conjugated magnetic microbeads (Miltenyi Biotech). The cells were then incubated at 4°C for 25 minutes followed by one wash with 8 mL of sorter buffer. Cells were next resuspended in 3 mL of sorter buffer and passed over a magnetized LS column (MACS Miltenyi Biotech). The column was washed with sorter buffer four times and then removed from the magnetic field. The bound cells were obtained by pushing 4.5 mL of sorter buffer through the column with a plunger. The resulting enriched fractions were centrifuged at 1500 rpm for 5 minutes at 4°C and resuspended in 0.05 mL of sorter buffer. The resuspended enriched cell fraction was stained with a cocktail of fluorochrome labeled antibodies specific for B220 (Invitrogen, Clone: RA3–6B2), CD11b (Invitrogen, Clone: M1/70), CD11c (Invitrogen, Clone: N41B), CD90.2 (Invitrogen, Clone: 30-H12), CD8 (BD Horizon, Clone: 53–6.7), CD4 (Invitrogen, Clone: RM4–4) and CD44 (Biolegend, Clone: IM7) at 4°C for 30 minutes. For intracellular staining for FoxP3, stained cells were fixed using fixation and permeabilization buffer kit from eBioscience (Cat# 00–5523-00) for 1 hour in the dark at 4°C. Cells were next stained with a 1:100 dilution of FoxP3 antibody (Invitrogen, Clone: FJK-16S) overnight at 4°C. After washing, cells were passed through a nylon mesh filter into a new FACS tube. 20,000 AccuCheck fluorescent counting beads (Life Technologies) were added to each sample for calculation of total epitope-specific T cell numbers. Samples were analyzed using an LSR II flow cytometer (BD Biosciences) and

FlowJo software (Tree Star). The number of tetramer positive events was multiplied by the beads ratio (expected beads divided by total beads in sample) to calculate the total number of tetramer positive cells in each mouse as described (Moon et al., 2009).

Flow cytometric T cell clonal deletion assay—Cleaved caspase 3 staining was performed using C57BL6 mice (5-week-old and 6-month-old) and mCat Tg mice (6-month-old) as described by Breed et al. (Breed et al., 2019). Single-cell suspensions were stained for 30 min at 4°C with the indicated antibodies. APC-conjugated anti-CD19 (6D5), CD25 (PC61), NK1.1 (PK136), TCRγ/∂ (GL3), and PerCPCy5.5-conjugated TCRβ (H57–597) were purchased from BioLegend (San Diego,CA). FITC-conjugated anti-CD5 (53–7.3) was purchased from Invitrogen (Waltham, MA). For staining with anti-cleaved caspase 3 (Asp175) (D3E9; Cell Signaling Technologies, Beverly, MA), cells were processed as quickly as possible following harvest to minimize cell death. Single cell suspensions were generated in FACS buffer by releasing the thymocytes from the harvested thymus by applying gentle mechanical force in circular motion to the thymus using back of the eppendorf tube. Following surface staining, cells were fixed with Cytofix/Cytoperm (BD Biosciences, San Jose, CA) for 30 minutes at 4°C. Cells were then washed with Perm/Wash buffer (BD Biosciences), and stained with anti–cleaved caspase 3 at a 1:200 dilution for 30 minutes at 23°C in the dark followed by staining with R-phycoerythrin goat anti-rabbit IgG (Thermofisher) for 30 minutes at 23°C in the dark. Samples were analyzed using an LSR II flow cytometer (BD Biosciences) and FlowJo software (Tree Star). Statistical analysis was performed with GraphPad Prism.

Microdissection—Intact thymuses were removed, immediately placed in ice-cold mounting medium (OCT, Tissue-Tek) and frozen in crushed dry ice. Transverse 20 μm sections were cut from the middle third of the tissue and mounted on PEN membrane slides (Leica). Sections selected for microdissection were chosen to have cortical regions 400–600um deep, medullary regions at least 200 μm deep, and symmetrical cortical/medullary borders. Tissue was fixed in cold acetone:ethanol (3:1 v/v), rehydrated through graded ethanol, stained with hematoxylin:ethanol (1:1), and dehydrated through graded ethanol. Slides were dried at room temperature and immediately used for microdissection on a Leica AS LMD system. RNA was isolated using RNAqueous Micro kits (Ambion). Each independent RNA pool included tissue from multiple sections and mice.

Microarray—Data described in this article will be submitted to the National Center for Biotechnology Information's Gene Expression Omnibus upon acceptance for publication. Microarray analysis for aged mCat Tg whole medulla samples was performed by the Genomics and Microarray Core at UT Southwestern. In brief, 0.2–1.0 μg of total RNA was used for 3′ *in vitro* one cycle target labeling (Affymetrix). Biotin-labeled cRNA probes were prepared as recommended by the manufacturer (Affymetrix), with oligo-dT primers, SuperScript, and BioArray High Yield RNA Transcript kits (Affymetrix). Fragmentation/hybridization to MOE430v2.0 arrays (Affymetrix) were performed according to Affymetrix protocols. Imaging was performed on an Affymetrix GeneChip Scanner 3000 per manufacturer's instructions. Raw data were analyzed using the Affymetrix Expression console. MIAME-compliant raw data have been deposited into the NCBI Gene Expression

Omnibus database (GEO: GSE189279). Young and aged WT whole medulla microarray data were previously published (GEO: GSE18281 and GEO: GSE132136). Expression values in Figure 2A represent PLIER normalized signals (see Table S1 in (Griffith et al., 2012)). Hierarchical clustering analysis was done in R (R: A language and environment for statistical computing, Foundation for Statistical Computing, Vienna, Austria. https://www.R-project.org/). Raw .cel files were processed with the mas5 function and present calls were generated using the mas5calls function, both from the R package affy (Gautier et al., 2004). The samples were quantile normalized using the normalizequantiles function from R package preprocessCore (https://github.com/bmbolstad/preprocessCore). For clustering, the probesets were restricted to those which received a present call in each of the samples in the young wild type OR old wild type OR old transgenic samples. The heatmap was generated using the heatmap.2 function from the R package gplots (gplots: Various R Programming Tools for Plotting Data. R package version 3.0.3. https://CRAN.R-project.org/package=gplots) using pearson correlation similarity as distance and average linkage as the clustering metric.

ELISpot—Mice were immunized by subcutaneous injection of 50 μg of ApoB peptide (GAYSNASSTESAS, Genescript) in 50 μL PBS emulsified in 50 μL CFA (CFA H37 Ra, BD) subcutaneously at the base of the tail. Two weeks later, CD4+ T cells were isolated from the spleen and inguinal lymph nodes and purified using a CD4+ T cell isolation kit (Stemcell). 2.5×10^5 CD4+ T cells were cultured with 2.5×10^5 irradiated B6 splenocytes and stimulated with 1.2 μM ApoB peptide (GAYSNASSTESAS) (in duplicate) for 24 hours in Multi-Screen-IP Filter Plate (Millipore) wells coated with anti-IFNγ (Clone# AN-18). After supernatants were removed, plates were incubated with biotinylated anti-mouse IFNγ (clone#R4–6A2) for 1.5 hours and, after washing, incubated with alkaline phosphatase-conjugated streptavidin. Plates were developed using nitroblue tetrazolium chloride (Sigma) and 5-bromo-4-chloro-3-indol phosphate p-toluidine salt (Sigma). Each well was scanned and counted using the CTL Immunospot (Cellular Technology).

Single cell sort of tetramer+ cells—The secondary lymphoid organs, including spleen and lymph nodes (inguinal, mesenteric, lumbar, axillary, brachial, and superficial) were harvested and processed in RPMI 1640 Medium (1x) (Hyclone Laboratories; Catalog number SH30027.01), 1M HEPES Buffer (Fisher Bioreagents; Catalog number BP299–500), and 10% Fetal Bovine Serum (FBS) (Corning; Reference number 35–010-CV) into a single cell suspension. The cells were incubated with Dasatinib (Tocris Biosciences) at a final concentration of 50 nM. The cells were then incubated at 37°C for 30 minutes. The cells were then incubated with a BD CD16/CD32 mouse Fc-Block (Clone: 2.4G2) and ApoBp:I-A^b-PE and APC-labeled tetramers for 1 hour at room temperature at a final concentration of 10 nM. After incubation, the cells were washed with a sorting buffer (MTH + 2% FBS + 0.1% sodium azide (NaN_3) (Acros Organics; Catalog number 447810250)). Anti-APC and anti-PE microbeads (Miltenyi Biotec; Catalog numbers 130–090-855; 130–048-801) were added to the tetramer-stained cells, incubated for 30 minutes, and washed with sorting buffer. The bound cells were then passed through an LS column (Miltenyi Biotec; Catalog number 130–042-401) on a QuadroMACS Separator (Miltenyi Biotec, Catalog number 130–091-051). The enriched cells were then stained with an antibody

cocktail consisting of antibodies specific for CD11b (eBioscience; 48–0112-82), CD11c (eBioscience; 48–0114-82), B220 (eBioscience; 48–0452-82), CD8a (BD Bioscience; 560776), CD44 (Biolegend; 103049), CD90.2 (eBioscience; 46–0903-82), CD4 (Biolegend; 100545) for 30 minutes on ice, subsequently washed, and resuspended in sorting buffer for flow cytometry analysis. Single tetramer positive cells were sorted on a BD FACSAria III Cell Sorter into 2x CellsDirect Lysis Buffer (Invitrogen, Catalog number 11753–100).

Primer name	Primer sequences (5′–3′)
FR4	Fw: ATGAATTCCAAGCGCCACAAG Rev: TTCCTGCCCGTTTGGGAC
CD44	Fw: AGCCCCTCCTGAAGAAGACT Rev: GCGAGTACCATCACGGTTGA
CD73	Fw: GCAAACATTAAGGCACGGGG Rev: ACGATGTCCACACCTCGAAC
IFNγ	Fw: CGGCACAGTCATTGAAAGCC Rev: TGCATCCTTTTTCGCCTTGC
GAPDH	Fw: TTTGGCATTGTGGAAGGGCT Rev: GTCAGATCCACGACGGACAC
FOXP3	Fw: TGCAGTTCCTTTGTGTCCGA Rev: ATAGTCACCCCAACACAGCG
HELIOS	Fw: CCCCTAATTGAGAGCAGCGA Rev: GCCCAATGCAAACCATGCC
Ki-67	Fw: AGTCTCTTGGCACTCACAGC Rev: ATGGATGCTCTCTTCGCAGG

q-RT-PCR from single cells—CellsDirect one-Step RT-PCR kit (Invitrogen, Catalog number 11753–100) was used for reverse transcription and specific target amplification (RT-PCR) for each single-cell and universal mouse total RNA of 200 pg. Quantitative PCR products were detected using Fluidigm BioMark HD system according to the protocol: Gene expression with the FlexSix IFC using Delta Gene assays (Fluidigm PN 100–7717 B1). GE Flex Six Fast PCR+Melt v1 program was used to collect the CT values. In each chip assay, universal mouse RNA (200 pg, cat# R4334566–1, BioChain, Newark, CA) and no template control (NTC) served as positive and negative controls. The cycling conditions were as follows: thermal mix at 25°C for 30 minutes, followed by 70°C for 60 minutes. After the thermal mix step, a hot start step at 95°C for 1 minute was performed. Once these steps were complete, 30 cycles of denaturing at 96°C for 5 seconds and annealing at 60°C for 20 seconds were performed. These steps included a ramp rate of 5.5°C/second. The final step included melting from 60 to 95°C for 3 second with a ramp rate of 1°C/second.

Analysis of single cell q-R-T-PCR results—Ct values >30 were set to 30. Any samples with ct values = 30 for GAPDH or CD4 were removed. Remaining data were plotted using the heatmap2 function from R package gplots with inferno color palette from viridisLite package. Individual genes from the same filtered data set were plotted using ggplot2 package with geom_violin(), geom_boxplot(), and geom_jitter().

Liver qPCR—About 0.15 g of the left lobe of the liver was homogenized in 2 mL TRIzol (ThermoFisher; Catalog number 15596026). Liver lysates were then centrifuged,

and the supernatant transferred and incubated with chloroform on ice for 10 minutes. After incubation, the lysates were centrifuged and the aqueous phase was extracted, to which an equal volume of isopropanol was added. The lysates were incubated at −20°C for 1 hour. Supernatants were discarded, and the pellets were washed with 1 mL of cold 75% ethanol, and centrifuged at 8000 g at 4°C, twice. The RNA pellet was resuspended in Nuclease Free Water (ThermoFisher; Catalog number AM9937). RNA concentration as determined using a ThermoFisher Nanodrop 2000 Specrophotometer. RNA was treated with DNAse I (NEB; Catalog number M0303S) at 37°C for 20 minutes. RNA was precipitated with 5M ammonium acetate (Invitrogen; Catalog number AM9070G) and 100% cold ethanol at −20°C overnight. After incubation, the precipitated RNA was centrifuged and washed. The RNA pellet was resuspended in Nuclease Free Water (ThermoFisher; Catalog number AM9937). RNA concentration was determined using a ThermoFisher Nanodrop 2000 Specrophotometer. Reverse transcription was performed using the SuperScript VILO cDNA Synthesis Kit (Invitrogen; Catalog number 11754050) according to the manufacturer's instructions. Quantitative PCR was performed using Taqman Gene Expression mix (Applied Biosystems; Catalog number 4370074) and ApoB primer probes (20x) (ThermoFisher; Mm01545156_m1) and run on a BioRad C1000 Thermocycler/CFX96 Real-Time System.

Flu infection—Mouse-adapted H1N1 influenza (A/Puerto Rico/8/1934 [PR8]) was provided by Dr. Marcia Blackman (Trudeau Institute, USA). Mice were anesthetized with light isoflurane anesthesia and 300 EID_{50} of PR8 suspended in 30 μL PBS was intranasally administered to the left nare of young (5 weeks) or older (6–6.5 months) C57BL/6J, mCAT or C57BL/6J NAC treated mice. Mice were monitored every two days post infection for 10 days and weighed.

Bronchoalveoloar lavage (BAL) and analysis of influenza-specific T cells—Upon euthanasia of influenza infected and/or uninfected mice, the trachea was exposed and a 2-inch-long (75% polyester, 25% cotton) thread was passed underneath the trachea using curved tweezers. An 18-gauge Insyte™ Autoguard™ shielded I.V. catheter (BD) was inserted into the upper trachea and secured using the thread. Bronchoalveoloar lavage (BAL) was removed by injecting and aspirating 0.8 mL of PBS containing Pierce™ protease inhibitors (Thermo Scientific; A32959) using a 1 mL PP/PE syringe (Sigma-Aldrich). BAL with protease inhibitors was placed in a separate tube on ice and the injection and aspiration procedure repeated six additional times using 1X PBS without protease inhibitors. The first aspirate containing protease inhibitors was centrifuged (660 RCF, 5 mins, 4°C) and supernatant stored at −80°C. Cells were then combined with other BAL removed with PBS and centrifuged (660 RCF, 5 mins, 4°C), and cells were resuspended in ice-cold FACS buffer (HBSS, 5% FBS, 0.5% DNAse (1 mg/mL), pH 7.2). Desatinib (Tocris Bioscience) was added to the cells at a final concentration of 50 nM and incubated 30 minutes at 37°C. After incubation, cells were cooled on ice for 5 minutes. Fc receptors were blocked with CD16/32 (93; eBioscience; #: 14–0161-81) for 10 minutes on ice followed by washing with FACS sorting buffer (HBSS +2% FBS +0.1% sodium azide). Cells were then stained with 0.5 mg of $NP_{366–374}/D^b$ (NP) and $PA_{224–233}/D^b$ (PA) tetramers and incubated while protected from light (1 hour at 25°C). Cells were then washed with sorting buffer, stained with CD11c-ef450 (N418; eBioscience), CD11b-ef450 (M1/70; eBioscience), B220-ef450 (RA3–

6B2; eBioscience), CD8-V500 (53–6.7; BD Biosciences) CD4-FITC (RM4–4; Invitrogen), CD90.2-PerCp-eFluor710 (30-H12; Invitrogen), and CD44-BV510 (IM7; Biolegend) on ice for 20 minutes. Cells were washed and suspended in sorting buffer for FACS analysis. NP-tetramer+ and PA-tetramer+ cells were analyzed on CD11c−CD11b−B220−CD90.2+CD8+ singlet lymphocytes using a BD LSRII flow cytometer (BD Biosciences) and BD FACSDiva and FlowJo flow cytometry analysis software (Tree Star).

QUANTIFICATION AND STATISTICAL ANALYSIS

Methods of statistical analysis, including Student's t-test (unpaired, two-tailed in all cases), one-way ANOVA are described in figure legends. Post-hoc tests applied are described in legends. $P < 0.05$ are interpreted as statistically significant. GraphPad Prism software was used for statistical analysis.

Supplementary Material

Refer to Web version on PubMed Central for supplementary material.

ACKNOWLEDGMENTS

We thank Dr. Marcia Blackman for helpful advice, the Trudeau Institute for providing the mouse-adapted H1N1 (A/Puerto Rico/8/1934 [PR8]) influenza virus, and the Molecular Biology Core Facility (MBCF) at Trudeau Institute for the production of the $NP_{366–374}/D^b$ and $PA_{224–233}/D^b$ tetramers. We thank Dr. Marc Jenkins for MHC class II tetramers and helpful discussions. Data were generated in the Flow Cytometry Shared Resource Facility, which is supported by UT Health San Antonio, NIH-NCI P30 CA054174–20 (CTRC at UTHSCSA), and UL1 TR001120 (CTSA grant). Data were also generated in the Bioanalytics and Single-Cell Core at UTHSCSA, which is supported by CPRIT grant (RP150600) and the Office of Vice President of Research, UTHSCSA. New microarray data were generated at the Microarray core at University of Texas Southwestern (UTSW). This work was supported by PHS grants R01AI121367 and R56AI153626, by the Conklyn Family Endowment in Autoimmune Research, and by funds from the UT Health San Antonio to A.V.G. A.K.H. was supported by PHS grants R01AI121367–04S1, R25GM095480, and T32AI138944. This work was supported in part by a grant to UT Health San Antonio from the Howard Hughes Medical Institute through the James H. Gilliam Fellowships for Advanced Study program (S.C.) and pilot funding under grant P30AG013319, San Antonio Nathan Shock Center. M.R. is supported by the IRACDA award K12 GM11 1726 and by the National Center for Advancing Translational Sciences of the National Institutes of Health under award number TL1TR002647.

REFERENCES

Ahmed M, Lanzer KG, Yager EJ, Adams PS, Johnson LL, and Blackman MA (2009). Clonal expansions and loss of receptor diversity in the naive CD8 T cell repertoire of aged mice. J. Immunol 182, 784–792. [PubMed: 19124721]

Aspinall R, Pitts D, Lapenna A, and Mitchell W (2010). Immunity in the elderly: the role of the thymus. J. Comp. Pathol 142, S111–S115. [PubMed: 19954794]

Baran-Gale J, Morgan MD, Maio S, Dhalla F, Calvo-Asensio I, Deadman ME, Handel AE, Maynard A, Chen S, Green F, et al. (2020). Ageing compromises mouse thymus function and remodels epithelial cell differentiation. Elife 9, e56221. [PubMed: 32840480]

Bhandoola A, von Boehmer H, Petrie HT, and Zuniga-Pflucker JC (2007). Commitment and developmental potential of extrathymic and intrathymic T cell precursors: plenty to choose from. Immunity 26, 678–689. [PubMed: 17582341]

Bredenkamp N, Jin X, Liu D, O'Neill KE, Manley NR, and Blackburn CC (2015). Construction of a functional thymic microenvironment from pluripotent stem cells for the induction of central tolerance. Regen. Med 10, 317–329. [PubMed: 25933240]

Bredenkamp N, Nowell CS, and Blackburn CC (2014). Regeneration of the aged thymus by a single transcription factor. Development 141, 1627–1637. [PubMed: 24715454]

Breed ER, Watanabe M, and Hogquist KA (2019). Measuring thymic clonal deletion at the population level. J. Immunol 202, 3226–3233. [PubMed: 31010850]

Brien JD, Uhrlaub JL, Hirsch A, Wiley CA, and Nikolich-Zugich J (2009). Key role of T cell defects in age-related vulnerability to West Nile virus. J. Exp. Med 206, 2735–2745. [PubMed: 19901080]

Britanova OV, Putintseva EV, Shugay M, Merzlyak EM, Turchaninova MA, Staroverov DB, Bolotin DA, Lukyanov S, Bogdanova EA, Mamedov IZ, et al. (2014). Age-related decrease in TCR repertoire diversity measured with deep and normalized sequence profiling. J. Immunol 192, 2689–2698. [PubMed: 24510963]

Callahan JE, Kappler JW, and Marrack P (1993). Unexpected expansions of CD8-bearing cells in old mice. J. Immunol 151, 6657–6669. [PubMed: 8258683]

Cepeda S, Cantu C, Orozco S, Xiao Y, Brown Z, Semwal MK, Venables T, Anderson MS, and Griffith AV (2018). Age-associated decline in thymic B cell expression of aire and aire-dependent self-antigens. Cell Rep. 22, 1276–1287. [PubMed: 29386114]

Cepeda S, and Griffith AV (2018). Thymic stromal cells: roles in atrophy and age-associated dysfunction of the thymus. Exp. Gerontol 105, 113–117. [PubMed: 29278750]

Chaudhry MS, Velardi E, Dudakov JA, and van den Brink MR (2016). Thymus: the next (re)generation. Immunol. Rev 271, 56–71. [PubMed: 27088907]

Chu YW, Schmitz S, Choudhury B, Telford W, Kapoor V, Garfield S, Howe D, and Gress RE (2008). Exogenous insulin-like growth factor 1 enhances thymopoiesis predominantly through thymic epithelial cell expansion. Blood 112, 2836–2846. [PubMed: 18658030]

Coder BD, Wang H, Ruan L, and Su DM (2015). Thymic involution perturbs negative selection leading to autoreactive T cells that induce chronic inflammation. J. Immunol 194, 5825–5837. [PubMed: 25957168]

Cooper GS, and Stroehla BC (2003). The epidemiology of autoimmune diseases. Autoimmun. Rev 2, 119–125. [PubMed: 12848952]

Derbinski J, Gabler J, Brors B, Tierling S, Jonnakuty S, Hergenhahn M, Peltonen L, Walter J, and Kyewski B (2005). Promiscuous gene expression in thymic epithelial cells is regulated at multiple levels. J. Exp. Med 202, 33–45. [PubMed: 15983066]

Dominguez-Gerpe L, and Rey-Mendez M (2003). Evolution of the thymus size in response to physiological and random events throughout life. Microsc. Res. Tech 62, 464–476. [PubMed: 14635139]

Dongre AR, Kovats S, deRoos P, McCormack AL, Nakagawa T, Paharkova-Vatchkova V, Eng J, Caldwell H, Yates JR 3rd, and Rudensky AY (2001). In vivo MHC class II presentation of cytosolic proteins revealed by rapid automated tandem mass spectrometry and functional analyses. Eur. J. Immunol 31, 1485–1494. [PubMed: 11465105]

Dudakov JA, Hanash AM, Jenq RR, Young LF, Ghosh A, Singer NV, West ML, Smith OM, Holland AM, Tsai JJ, et al. (2012). Interleukin-22 drives endogenous thymic regeneration in mice. Science 336, 91–95. [PubMed: 22383805]

Ernst DN, Hobbs MV, Torbett BE, Glasebrook AL, Rehse MA, Bottomly K, Hayakawa K, Hardy RR, and Weigle WO (1990). Differences in the expression profiles of CD45RB, Pgp-1, and 3G11 membrane antigens and in the patterns of lymphokine secretion by splenic CD4+ T cells from young and aged mice. J. Immunol 145, 1295–1302. [PubMed: 1974562]

Fahy GM, Brooke RT, Watson JP, Good Z, Vasanawala SS, Maecker H, Leipold MD, Lin DTS, Kobor MS, and Horvath S (2019). Reversal of epigenetic aging and immunosenescent trends in humans. Aging Cell 18, e13028. [PubMed: 31496122]

Foss DL, Donskoy E, and Goldschneider I (2001). The importation of hematogenous precursors by the thymus is a gated phenomenon in normal adult mice. J. Exp. Med 193, 365–374. [PubMed: 11157056]

Garfin PM, Min D, Bryson JL, Serwold T, Edris B, Blackburn CC, Richie ER, Weinberg KI, Manley NR, Sage J, and Viatour P (2013). Inactivation of the RB family prevents thymus involution and promotes thymic function by direct control of Foxn1 expression. J. Exp. Med 210, 1087–1097. [PubMed: 23669396]

Gautier L, Cope L, Bolstad BM, and Irizarry RA (2004). affy–analysis of Affymetrix GeneChip data at the probe level. Bioinformatics 20, 307–315. [PubMed: 14960456]

Gies V, Guffroy A, Danion F, Billaud P, Keime C, Fauny JD, Susini S, Soley A, Martin T, Pasquali JL, et al. (2017). B cells differentiate in human thymus and express AIRE. J. Allergy Clin. Immunol 139, 1049–1052 e1012. [PubMed: 27864026]

Gil A, Yassai MB, Naumov YN, and Selin LK (2015). Narrowing of human influenza A virus-specific T cell receptor alpha and beta repertoires with increasing age. J. Virol 89, 4102–4116. [PubMed: 25609818]

Goldschneider I, Komschlies KL, and Greiner DL (1986). Studies of thymocytopoiesis in rats and mice. I. Kinetics of appearance of thymocytes using a direct intrathymic adoptive transfer assay for thymocyte precursors. J. Exp. Med 163, 1–17. [PubMed: 3510267]

Goronzy JJ, and Weyand CM (2012). Immune aging and autoimmunity. Cell Mol. Life Sci 69, 1615–1623. [PubMed: 22466672]

Griffith AV, Fallahi M, Nakase H, Gosink M, Young B, and Petrie HT (2009). Spatial mapping of thymic stromal microenvironments reveals unique features influencing T lymphoid differentiation. Immunity 31, 999–1009. [PubMed: 20064453]

Griffith AV, Fallahi M, Venables T, and Petrie HT (2012). Persistent degenerative changes in thymic organ function revealed by an inducible model of organ regrowth. Aging Cell 11, 169–177. [PubMed: 22103718]

Griffith AV, Venables T, Shi J, Farr A, van Remmen H, Szweda L, Fallahi M, Rabinovitch P, and Petrie HT (2015). Metabolic damage and premature thymus aging caused by stromal catalase deficiency. Cell Rep. 12, 1071–1079. [PubMed: 26257169]

Hale JS, Boursalian TE, Turk GL, and Fink PJ (2006). Thymic output in aged mice. Proc. Natl. Acad. Sci. U.S.A 103, 8447–8452. [PubMed: 16717190]

Hartwig M, and Steinmann G (1994). On a causal mechanism of chronic thymic involution in man. Mech. Ageing Dev. 75, 151–156. [PubMed: 7823637]

Hassler T, Urmann E, Teschner S, Federle C, Dileepan T, Schober K, Jenkins MK, Busch DH, Hinterberger M, and Klein L (2019). Inventories of naive and tolerant mouse CD4 T cell repertoires reveal a hierarchy of deleted and diverted T cell receptors. Proc. Natl. Acad. Sci. U.S.A 116, 18537–18543. [PubMed: 31451631]

Haynes BF, Sempowski GD, Wells AF, and Hale LP (2000). The human thymus during aging. Immunol. Res 22, 253–261. [PubMed: 11339360]

Haynes L, Eaton SM, Burns EM, Randall TD, and Swain SL (2003). CD4 T cell memory derived from young naive cells functions well into old age, but memory generated from aged naive cells functions poorly. Proc. Natl. Acad. Sci. U.S.A 100, 15053–15058. [PubMed: 14657384]

Heng TS, Reiseger JJ, Fletcher AL, Leggatt GR, White OJ, Vlahos K, Frazer IH, Turner SJ, and Boyd RL (2012). Impact of sex steroid ablation on viral, tumour and vaccine responses in aged mice. PLoS ONE 7, e42677. [PubMed: 22880080]

Hermansson A, Ketelhuth DF, Strodthoff D, Wurm M, Hansson EM, Nicoletti A, Paulsson-Berne G, and Hansson GK (2010). Inhibition of T cell response to native low-density lipoprotein reduces atherosclerosis. J. Exp. Med 207, 1081–1093. [PubMed: 20439543]

Hu DY, Yap JY, Wirasinha RC, Howard DR, Goodnow CC, and Daley SR (2016). A timeline demarcating two waves of clonal deletion and Foxp3 upregulation during thymocyte development. Immunol. Cell Biol 94, 357–366. [PubMed: 26510893]

Hun M, Barsanti M, Wong K, Ramshaw J, Werkmeister J, and Chidgey AP (2017). Native thymic extracellular matrix improves in vivo thymic organoid T cell output, and drives in vitro thymic epithelial cell differentiation. Biomaterials 118, 1–15. [PubMed: 27940379]

Kalekar LA, and Mueller DL (2017). Relationship between CD4 regulatory T cells and anergy in vivo. J. Immunol 198, 2527–2533. [PubMed: 28320913]

Ki S, Park D, Selden HJ, Seita J, Chung H, Kim J, Iyer VR, and Ehrlich LI (2014). Global transcriptional profiling reveals distinct functions of thymic stromal subsets and age-related changes during thymic involution. Cell Rep. 9, 402–415. [PubMed: 25284794]

Kim MJ, Miller CM, Shadrach JL, Wagers AJ, and Serwold T (2015). Young, proliferative thymic epithelial cells engraft and function in aging thymuses. J. Immunol 194, 4784–4795. [PubMed: 25870244]

Kimura T, Kobiyama K, Winkels H, Tse K, Miller J, Vassallo M, Wolf D, Ryden C, Orecchioni M, Dileepan T, et al. (2018). Regulatory CD4(+) T cells recognize major histocompatibility complex class II molecule-restricted peptide epitopes of Apolipoprotein B. Circulation 138, 1130–1143. [PubMed: 29588316]

Kimura T, Tse K, McArdle S, Gerhardt T, Miller J, Mikulski Z, Sidney J, Sette A, Wolf D, and Ley K (2017). Atheroprotective vaccination with MHC-II-restricted ApoB peptides induces peritoneal IL-10-producing CD4 T cells. Am. J. Physiol. Heart Circ. Physiol 312, H781–H790. [PubMed: 28087520]

Kimura T, Tse K, Sette A, and Ley K (2015). Vaccination to modulate atherosclerosis. Autoimmunity 48, 152–160. [PubMed: 25683179]

Klein L, Kyewski B, Allen PM, and Hogquist KA (2014). Positive and negative selection of the T cell repertoire: what thymocytes see (and don't see). Nat. Rev. Immunol 14, 377–391. [PubMed: 24830344]

Koltsova EK, Garcia Z, Chodaczek G, Landau M, McArdle S, Scott SR, von Vietinghoff S, Galkina E, Miller YI, Acton ST, and Ley K (2012). Dynamic T cell-APC interactions sustain chronic inflammation in atherosclerosis. J. Clin. Invest 122, 3114–3126. [PubMed: 22886300]

Lee JB, Oelke M, Ramachandra L, Canaday DH, and Schneck JP (2011). Decline of influenza-specific CD8+ T cell repertoire in healthy geriatric donors. Immun. Ageing 8, 6. [PubMed: 21846352]

Lepletier A, Chidgey AP, and Savino W (2015). Perspectives for improvement of the thymic microenvironment through manipulation of thymic epithelial cells: a mini-review. Gerontology 61, 504–514. [PubMed: 25765703]

Lo Sasso G, Schlage WK, Boue S, Veljkovic E, Peitsch MC, and Hoeng J (2016). The Apoe(−/−) mouse model: a suitable model to study cardiovascular and respiratory diseases in the context of cigarette smoke exposure and harm reduction. J. Transl Med 14, 146. [PubMed: 27207171]

Luc S, Luis TC, Boukarabila H, Macaulay IC, Buza-Vidas N, Bouriez-Jones T, Lutteropp M, Woll PS, Loughran SJ, Mead AJ, et al. (2012). The earliest thymic T cell progenitors sustain B cell and myeloid lineage potential. Nat. Immunol 13, 412–419. [PubMed: 22344248]

Luis TC, Luc S, Mizukami T, Boukarabila H, Thongjuea S, Woll PS, Azzoni E, Giustacchini A, Lutteropp M, Bouriez-Jones T, et al. (2016). Initial seeding of the embryonic thymus by immune-restricted lympho-myeloid progenitors. Nat. Immunol 17, 1424–1435. [PubMed: 27695000]

Majumdar S, and Nandi D (2017). Thymic atrophy: experimental studies and therapeutic interventions. Scand J. Immunol 87, 4–14. [PubMed: 28960415]

Masters AR, Haynes L, Su DM, and Palmer DB (2017). Immune senescence: significance of the stromal microenvironment. Clin. Exp. Immunol 187, 6–15. [PubMed: 27529161]

Montecino-Rodriguez E, Berent-Maoz B, and Dorshkind K (2013). Causes, consequences, and reversal of immune system aging. J. Clin. Invest 123, 958–965. [PubMed: 23454758]

Montecino-Rodriguez E, Clark R, and Dorshkind K (1998). Effects of insulin-like growth factor administration and bone marrow transplantation on thymopoiesis in aged mice. Endocrinology 139, 4120–4126. [PubMed: 9751491]

Moon JJ, Chu HH, Hataye J, Pagan AJ, Pepper M, McLachlan JB, Zell T, and Jenkins MK (2009). Tracking epitope-specific T cells. Nat. Protoc 4, 565–581. [PubMed: 19373228]

Moon JJ, Chu HH, Pepper M, McSorley SJ, Jameson SC, Kedl RM, and Jenkins MK (2007). Naive CD4(+) T cell frequency varies for different epitopes and predicts repertoire diversity and response magnitude. Immunity 27, 203–213. [PubMed: 17707129]

Muller L, and Pawelec G (2015). As we age: does slippage of quality control in the immune system lead to collateral damage? Ageing Res. Rev 23, 116–123. [PubMed: 25676139]

Nelson RW, Beisang D, Tubo NJ, Dileepan T, Wiesner DL, Nielsen K, Wuthrich M, Klein BS, Kotov DI, Spanier JA, et al. (2015). T cell receptor cross-reactivity between similar foreign and self peptides influences naive cell population size and autoimmunity. Immunity 42, 95–107. [PubMed: 25601203]

Nikolich-Zugich J, and Rudd BD (2010). Immune memory and aging: an infinite or finite resource? Curr. Opin. Immunol 22, 535–540. [PubMed: 20674320]

Palmer S, Albergante L, Blackburn CC, and Newman TJ (2018). Thymic involution and rising disease incidence with age. Proc. Natl. Acad. Sci. U S A 115, 1883–1888. [PubMed: 29432166]

Parent AV, Russ HA, Khan IS, LaFlam TN, Metzger TC, Anderson MS, and Hebrok M (2013). Generation of functional thymic epithelium from human embryonic stem cells that supports host T cell development. Cell Stem Cell 13, 219–229. [PubMed: 23684540]

Posnett DN, Sinha R, Kabak S, and Russo C (1994). Clonal populations of T cells in normal elderly humans: the T cell equivalent to “benign monoclonal gammapathy”. J. Exp. Med 179, 609–618. [PubMed: 8294871]

Prockop SE, and Petrie HT (2004). Regulation of thymus size by competition for stromal niches among early T cell progenitors. J. Immunol 173, 1604–1611. [PubMed: 15265888]

Reynaldi A, Smith NL, Schlub TE, Tabilas C, Venturi V, Rudd BD, and Davenport MP (2019). Fate mapping reveals the age structure of the peripheral T cell compartment. Proc. Natl. Acad. Sci. U S A 116, 3974–3981. [PubMed: 30765525]

Rode I, and Boehm T (2012). Regenerative capacity of adult cortical thymic epithelial cells. Proc. Natl. Acad. Sci. U S A 109, 3463–3468. [PubMed: 22331880]

Rossi SW, Jeker LT, Ueno T, Kuse S, Keller MP, Zuklys S, Gudkov AV, Takahama Y, Krenger W, Blazar BR, and Hollander GA (2007). Keratinocyte growth factor (KGF) enhances postnatal T-cell development via enhancements in proliferation and function of thymic epithelial cells. Blood 109, 3803–3811. [PubMed: 17213286]

Sanchez M, Lindroth K, Sverremark E, Gonzalez Fernandez A, and Fernandez C (2001). The response in old mice: positive and negative immune memory after priming in early age. Int. Immunol 13, 1213–1221. [PubMed: 11581166]

Schriner SE, Linford NJ, Martin GM, Treuting P, Ogburn CE, Emond M, Coskun PE, Ladiges W, Wolf N, Van Remmen A, et al. (2005). Extension of murine life span by overexpression of catalase targeted to mitochondria. Science 308, 1909–1911. [PubMed: 15879174]

Sempowski GD, Gooding ME, Liao HX, Le PT, and Haynes BF (2002). T cell receptor excision circle assessment of thymopoiesis in aging mice. Mol. Immunol 38, 841–848. [PubMed: 11922942]

Shah NJ, Mao AS, Shih TY, Kerr MD, Sharda A, Raimondo TM, Weaver JC, Vrbanac VD, Deruaz M, Tager AM, et al. (2019). An injectable bone marrow-like scaffold enhances T cell immunity after hematopoietic stem cell transplantation. Nat. Biotechnol 37, 293–302. [PubMed: 30742125]

Shaw MK, Tse KY, Zhao X, Welch K, Eitzman DT, Thipparthi RR, Montgomery PC, Thummel R, and Tse HY (2017). T-cells specific for a self-peptide of ApoB-100 exacerbate aortic atheroma in murine atherosclerosis. Front. Immunol 8, 95. [PubMed: 28280493]

Shukla S, Langley MA, Singh J, Edgar JM, Mohtashami M, Zuniga-Pflucker JC, and Zandstra PW (2017). Progenitor T-cell differentiation from hematopoietic stem cells using delta-like-4 and VCAM-1. Nat. Methods 14, 531–538. [PubMed: 28394335]

Smithey MJ, Li G, Venturi V, Davenport MP, and Nikolich-Zugich J (2012). Lifelong persistent viral infection alters the naive T cell pool, impairing CD8 T cell immunity in late life. J. Immunol 189, 5356–5366. [PubMed: 23087407]

Stacy S, Infante AJ, Wall KA, Krolick K, and Kraig E (2003). Recall immune memory: a new tool for generating late onset autoimmune myasthenia gravis. Mech. Ageing Dev 124, 931–940. [PubMed: 14499498]

Steinmann GG, Klaus B, and Muller-Hermelink HK (1985). The involution of the ageing human thymic epithelium is independent of puberty. A morphometric study. Scand. J. Immunol 22, 563–575. [PubMed: 4081647]

Sun X, Xu J, Lu H, Liu W, Miao Z, Sui X, Liu H, Su L, Du W, He Q, et al. (2013). Directed differentiation of human embryonic stem cells into thymic epithelial progenitor-like cells reconstitutes the thymic microenvironment in vivo. Cell Stem Cell 13, 230–236. [PubMed: 23910085]

Sutherland JS, Goldberg GL, Hammett MV, Uldrich AP, Berzins SP, Heng TS, Blazar BR, Millar JL, Malin MA, Chidgey AP, and Boyd RL (2005). Activation of thymic regeneration in mice and humans following androgen blockade. J. Immunol 175, 2741–2753. [PubMed: 16081852]

Tse K, Gonen A, Sidney J, Ouyang H, Witztum JL, Sette A, Tse H, and Ley K (2013). Atheroprotective vaccination with MHC-II restricted peptides from ApoB-100. Front. Immunol 4, 493. [PubMed: 24416033]

Utsuyama M, Hirokawa K, Kurashima C, Fukayama M, Inamatsu T, Suzuki K, Hashimoto W, and Sato K (1992). Differential age-change in the numbers of CD4+CD45RA+ and CD4+CD29+ T cell subsets in human peripheral blood. Mech. Ageing Dev 63, 57–68. [PubMed: 1376382]

Venables T, Griffith AV, DeAraujo A, and Petrie HT (2019). Dynamic changes in epithelial cell morphology control thymic organ size during atrophy and regeneration. Nat. Commun 10, 4402. [PubMed: 31562306]

Wolf D, Gerhardt T, Winkels H, Michel NA, Pramod AB, Ghosheh Y, Brunel S, Buscher K, Miller J, McArdle S, et al. (2020). Pathogenic autoimmunity in atherosclerosis evolves from initially protective Apolipoprotein B100-reactive CD4(+) T-regulatory cells. Circulation 142, 1279–1293. [PubMed: 32703007]

Yager EJ, Ahmed M, Lanzer K, Randall TD, Woodland DL, and Blackman MA (2008). Age-associated decline in T cell repertoire diversity leads to holes in the repertoire and impaired immunity to influenza virus. J. Exp. Med 205, 711–723. [PubMed: 18332179]

Yamaguchi T, Hirota K, Nagahama K, Ohkawa K, Takahashi T, Nomura T, and Sakaguchi S (2007). Control of immune responses by antigen-specific regulatory T cells expressing the folate receptor. Immunity 27, 145–159. [PubMed: 17613255]

Yoshida K, Cologne JB, Cordova K, Misumi M, Yamaoka M, Kyoizumi S, Hayashi T, Robins H, and Kusunoki Y (2017). Aging-related changes in human T-cell repertoire over 20years delineated by deep sequencing of peripheral T-cell receptors. Exp. Gerontol 96, 29–37. [PubMed: 28535950]

Highlights

- Aging impairs central T cell tolerance induction in the thymus
- Decreased autoantigen expression in thymus correlates with increasing autoreactivity
- Catalase expression mitigates age-associated waning of flu-specific T cells
- Redox status effect on T cell selection varies across TCR specificities

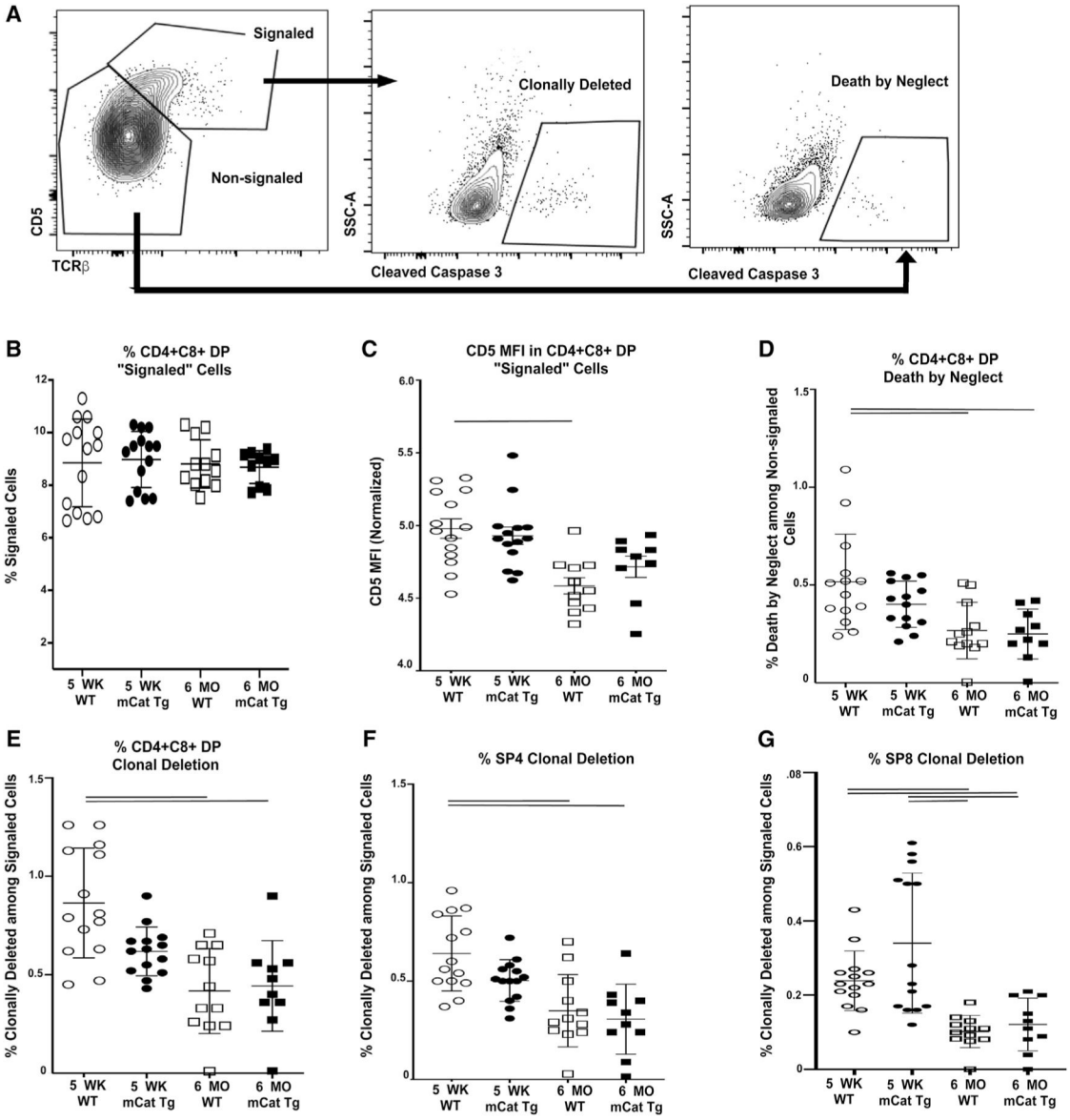

Figure 1. Negative selection of T cells is impaired by 6 months of age at the population level in the thymus of WT mice and is not restored when atrophy is delayed by reducing oxidative damage

(A) The gating strategy used to identify (viable singlet, Lineage$^-$ [CD25$^-$, NK1.1$^-$, CD19$^-$, TCRγ/δ^-]) T cells undergoing clonal deletion and death by neglect.

(B) The frequencies of CD5$^+$ TCRβ^+ signaled thymocytes among CD4$^+$CD8$^+$ DP cells in 6-month-old WT (n = 12) and 6-month-old mCat Tg mice (n = 10) are similar to 5-week-old WT (n = 14) and 5-week-old mCat Tg (n = 14).

(C) Plots represent CD5 median fluorescence intensity (MFI) of CD4$^+$CD8$^+$ DP "signaled" thymocytes (normalized to non-signaled) gated as in (A).

(D) Plots represent the frequency of cleaved caspase-3$^+$ cells among CD5$^-$TCRβ^- CD4$^+$CD8 DP thymocytes undergoing death by neglect.

(E) The frequency of cleaved caspase-3$^+$ cells among CD5$^+$TCRβ^+ CD4$^+$CD8$^+$ DP thymocytes undergoing clonal deletion.

(F) The frequency of cleaved caspase-3^+ cells among $CD5^+TCR\beta^+$ $CD4^+CD8^-$ SP4 thymocytes undergoing clonal deletion.
(G) The frequency of cleaved caspase-3^+ cells among $CD5^+TCR\beta^+$ $CD4^-CD8^+$ SP8 thymocytes undergoing clonal deletion.
Horizontal bars indicate one-way ANOVA Fisher's least significant difference (LSD) $p < 0.05$. Symbols represent individual mice. Mean and SEM are indicated by bars in each group. See also Figure S1.

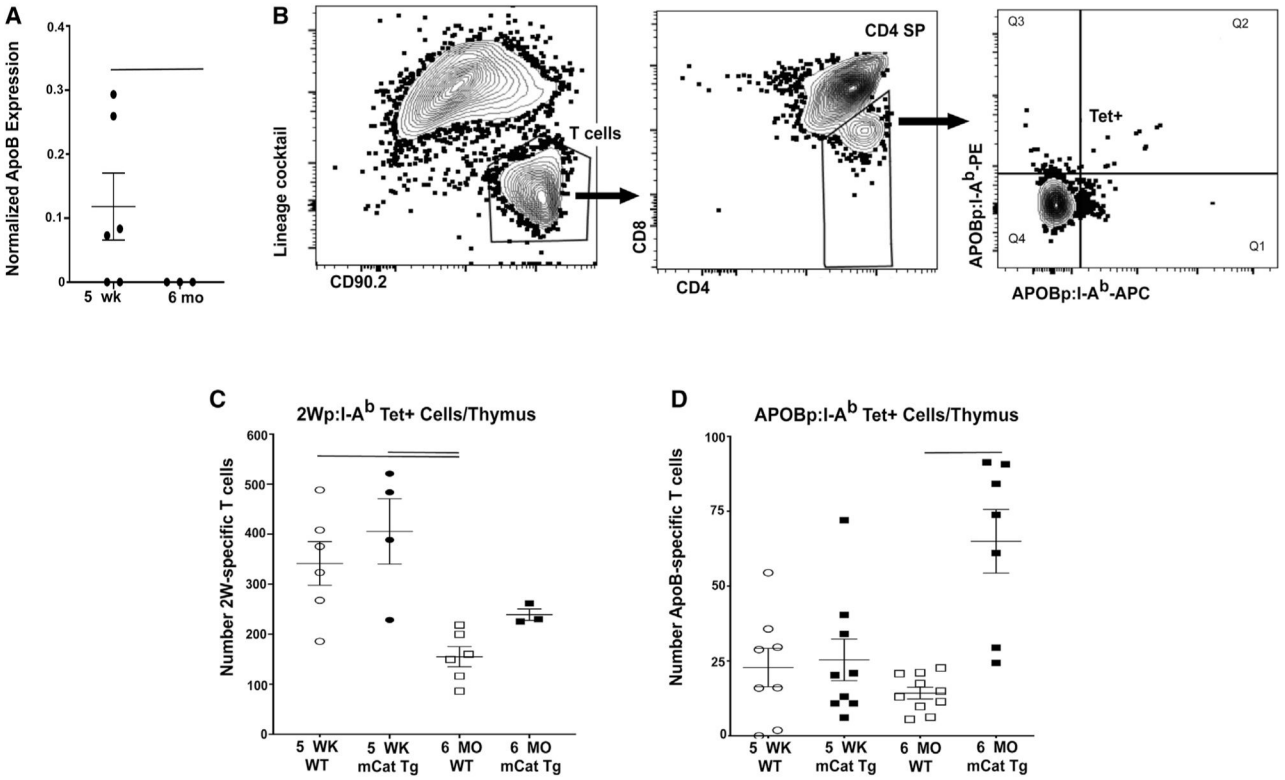

Figure 2. Negative selection of ApoB-specific CD4 T cells decreases by 6 months of age and is not restored when thymic atrophy is delayed by reducing oxidative damage

(A) The expression of a model TRA, ApoB (PLIER normalized M430_2 expression values, probe set 1455593_at) in microdissected whole medullary tissue from young (5-week-old; n = 7) and older (12-month-old; n = 3) mice from a previously published dataset (see Table S1; Griffith et al., 2012). Expression declines in aged mice (two-tailed Student's t test for unpaired samples; $p < 0.02$). Mean and SEM are indicated by horizontal lines.

(B) Representative gating strategy used to identify tetramer-positive cells from thymus following enrichment with the appropriate tetramers labeled with APC or phycoerythrin (PE). Tetramer-binding cells were identified among SP $CD4^+$ T cells ($Lineage^-$ [$B220^-$, $CD11b^-$, $CD11c^-$], $CD90^+$, $CD8^-$, $CD4^+$).

(C) The total number of T cells in thymus that recognize a representative foreign antigen derived from the I-Ea chain designated "2W". Total numbers of tetramer-binding $CD4^+$ T cells per thymus binding 2W:I-A^b tetramers decrease proportionally to total thymus size in 6-month-old WT (n = 6) relative to 5 weeks old (n = 6). 2W-specific T cells are not altered in young (n = 4) or older (n = 3) mCat Tg mice relative to age-matched WT.

(D) The total number of ApoB:I-A^b tetramer-binding T cells per thymus in 6-month-old WT thymuses (n = 10) relative to 5-week-old WT thymuses (n = 8) and mCat Tg thymuses (n = 9) and the 6-month-old mCat Tg thymus (n = 7).

Horizontal bars indicate one-way ANOVA Fisher's LSD; $p < 0.05$. Symbols represent individual mice. Mean and SEM are indicated by bars in each group. See also Figure S2 and Table S1.

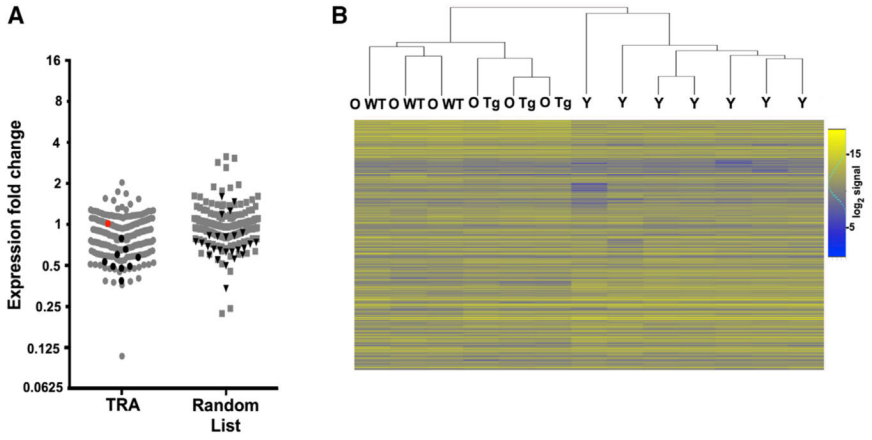

Figure 3. Diminished TRA expression is not restored by reducing oxidative stress

(A) Relative expression (12-month-old mCat Tg/12-month-old WT) of TRAs. An informatically established objective list of 238 probe sets representing tissue-restricted antigens expressed by thymic medullary stromal cells was used to compare gene expression levels in 12-month-old mCat Tg and 12-month-old WT whole medullary tissue (Mas5 M430_2 expression values from 12-month-old [n = 3] mice from a previously published dataset; see Table S1; Griffith et al., 2012) and 12-month-old (n = 3) mCat Tg mice. Statistically significant (two-tailed Student's t test for unpaired samples) changes in expression are indicated by black dots, while those that were not statistically significant are indicated in gray. ApoB ratio is indicated in red.

(B) Unsupervised two-dimensional clustering of absolute Mas5 values ($\log_2$) for all genes expressed (called present in all samples in any of the three groups) in young (5 week; n = 7 chips) WT and old (12 month; n = 3) WT microdissected whole medulla (WM), which were previously published datasets (Griffith et al., 2012) and a newly generated dataset derived from old (12 month; n = 3) mCat Tg (Tg) microdissected WM.

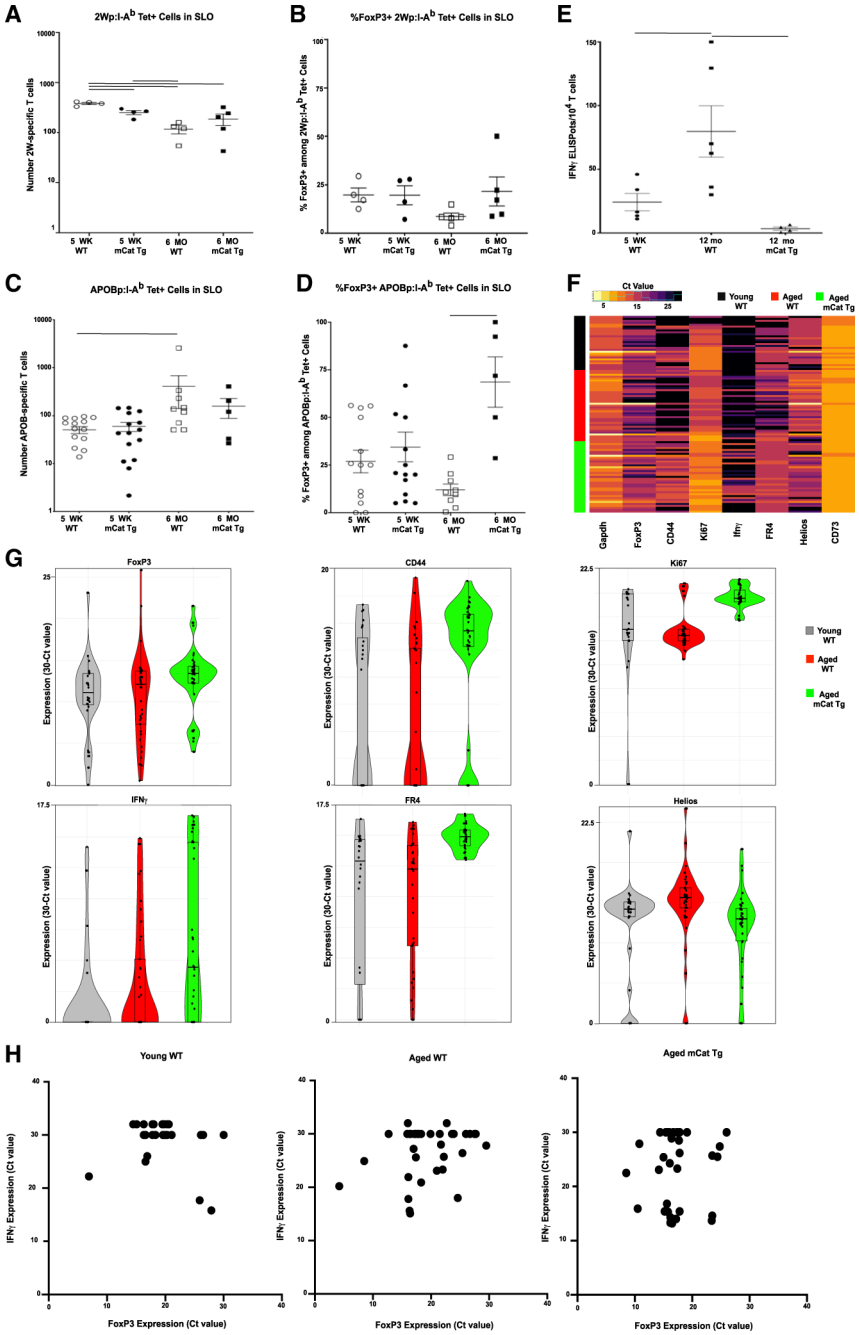

Figure 4. Age-associated increases in peripheral T cell responsiveness to ApoB in WT mice are rescued in catalase transgenic mice

(A) The plot represents the total number of T cells in the secondary lymphoid organs (SLOs) (spleen and lymph nodes) recognizing a representative foreign antigen designated 2W. Total numbers of $CD4^+$ T cells in the SLO binding 2W:I-A^b tetramer in 5-week-old WT (n = 4), 5-week-old mCat Tg (n = 4), 6-month-old WT (n = 4), and 6-month-old mCat Tg are shown (n = 5).

(B) Frequency of $FoxP3^+$ cells among 2W:I-A^b tetramer binding $CD4^+$ T cells in the SLOs of mice in (A).

(C) The total number of ApoB:I-A^b tetramer-binding T cells in the SLOs of individual mice in 6-month-old WT (n = 9) and 5-week-old WT (n = 16). The number of ApoB-specific T cells in the 6-month-old mCat Tg (n = 5) and 5-week-old mCat Tg (n = 15) is not significantly different from other groups.
(D) Frequency of $FoxP3^+$ cells among ApoB:I-A^b tetramer-binding $CD4^+$ T cells in the SLOs of 5-week-old WT (n = 13), 5-week-old mCat Tg (n = 15), 6-month-old WT (n = 9), and 6-month-old mCat Tg mice (n = 5).
(E) The ELISpot assay was used to measure effector T cells responding to ApoB immunization 14 days after subcutaneous injection of ApoB peptide emulsified in CFA. IFN-γ-secreting T cells increased in WT 12-month-old mice (n = 6) relative to 5-week-old WT mice (n = 5). Expression of the mCat transgene in 12-month-old mCat Tg mice (n = 4) rescued this increase.
(F) Heatmap represents single-cell gene expression (Ct values) in ApoB-specific T cells from three young (4- to 8-week-old) WT mice, five aged (12- to 18-month-old) WT mice, and five aged (12- to 18-month-old) mCat Tg mice.
(G) Violin plots represent gene expression (30-Ct value) for a subset of transcripts in (F). Each dot represents a single cell. Boxes indicate 25^{th}, 50^{th}, and 75^{th} percentiles.
(H) Each dot represents expression (Ct value) of IFN-γ (y axis) and FoxP3 (x axis) for a single cell from the indicated group.
(A–D) Horizontal bars indicate one-way ANOVA Fisher's LSD; $p < 0.05$. Symbols represent individual mice. Mean and SEM are indicated by bars in each group. See also Figure S3.

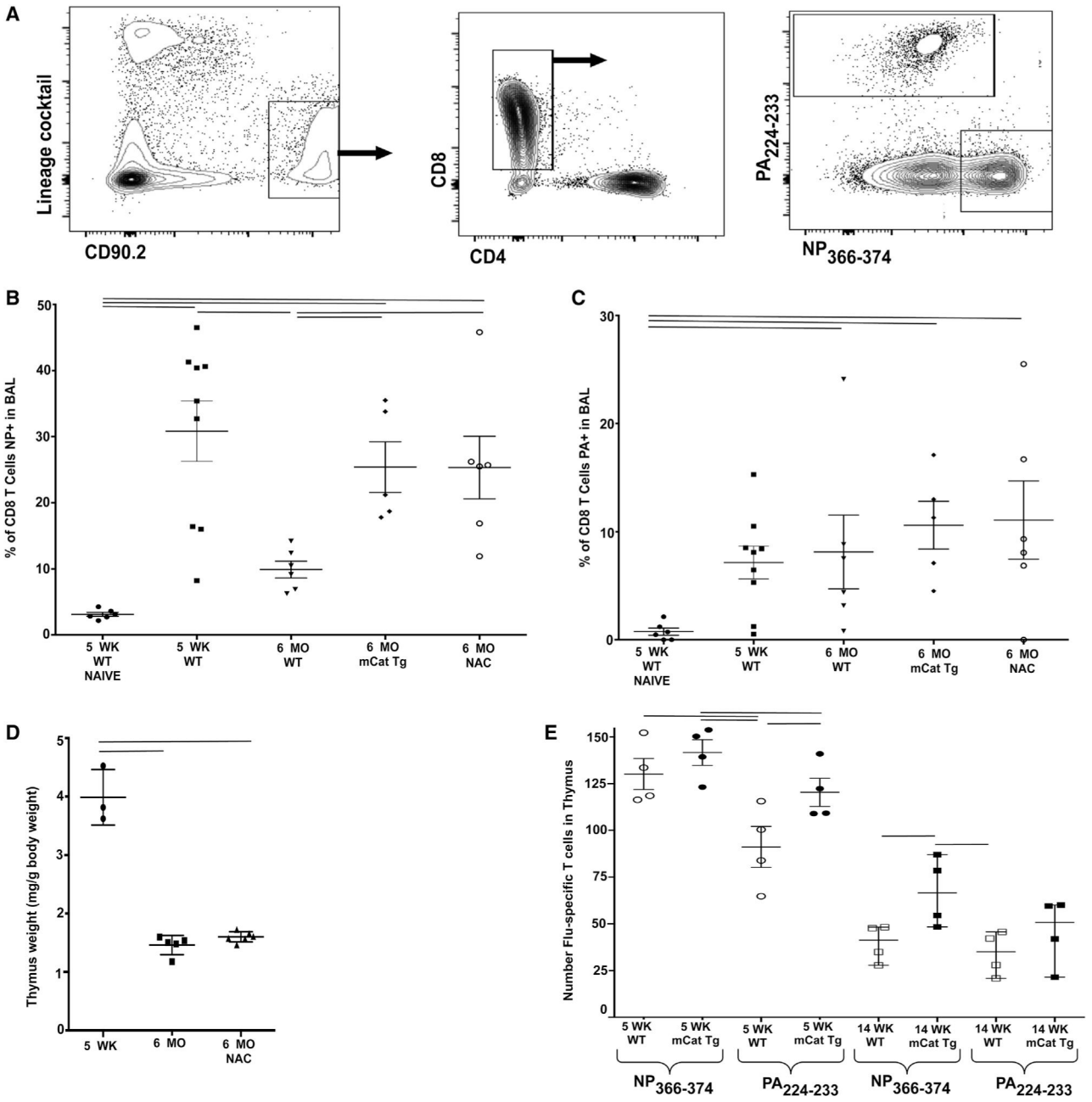

Figure 5. Dietary and genetic antioxidant supplementation rescues CD8 T cell responsiveness to the influenza virus immunodominant epitope, $NP_{366–374}$, at 6 months of age

(A) A representative gating strategy used to identify tetramer-positive cells from bronchoalveolar lavage (BAL). BAL cells were stained with APC-conjugated $NP_{366–374}/D^b$ tetramer, PE-conjugated $PA_{224–233}/D^b$ tetramer, anti-CD8-fluorescein isothiocyanate (FITC), and PE-Cy5-conjugated anti-CD19 and anti-CD4 (“lineage cocktail” channel).

(B) BAL was harvested 10 days after influenza virus infection (5 WK WT; n = 9) or from naive individual young mice (5 WK NAIVE; n = 6) and older mice given either control untreated water (6 MO WT; n = 6) or NAC-supplemented water from weaning (6 MO NAC; n = 6) and older mCat Tg mice (6 MO mCat Tg; n = 5). Symbols represent individual

mice. Horizontal bars indicate one-way ANOVA; $p < 0.05$. Mean and SEM are indicated by horizontal bars in each group.

(C) Frequencies of PA-specific CD8 T cells after enrichment in BAL are displayed. Symbols represent individual mice. Horizontal bars indicate one-way ANOVA; $p < 0.05$. Mean and SEM are indicated by horizontal bars in each group: 5 WK WT NAIVE animals (n = 6); 5 WK WT animals post-infection (n = 9); 6 MO WT animals post-infection (n = 6); 6 MO mCat Tg animals post-infection (n = 5); and 6 MO NAC animals post-infection (n = 5).

(D) Drinking water supplemented with 15 mg/mL NAC was given from weaning, and thymus weight was measured at 6 months in treated (n = 6) and untreated control mice (n = 5) and in young untreated controls at 5 weeks (n = 3). Mice supplemented with NAC did not exhibit an increase in thymus size when compared with that of the control mice of the same age, indicating that the impact of NAC on thymus size is lost sometime between 10 weeks of age and 6 months of age.

(E) Total numbers of NP- and PA-specific T cells in the thymus of young WT (5 WK; n = 4) and mCat Tg (n = 4) mice and 14-week-old WT (n = 4) and mCat Tg (n = 4) mice. Symbols represent individual mice.

Horizontal bars indicate one-way ANOVA Fisher's LSD; $p < 0.05$. In (E), NP- and PA-specific T cell numbers were significantly decreased ($p < 0.05$) in all 14-week thymus samples relative to 5-week samples from the same genotype, but these bars were omitted for clarity. Mean and SEM are indicated by horizontal bars.

KEY RESOURCES TABLE

REAGENT or RESOURCE	SOURCE	IDENTIFIER
Antibodies		
anti-B220 (Clone: RA3-6B2)	Invitrogen	Cat# 48-0452-82; RRID: AB_1548761
anti-CD11b (Clone: M1/70)	Invitrogen	Cat# 48-0112-82; RRID: AB_1582236
anti-CD11c (Clone: N41B)	Invitrogen	Cat# 48-0114-82; RRID: AB_1548654
anti-CD90.2 (Clone: 30-H12)	Invitrogen	Cat# 46-0903-82; RRID: AB_10670882
anti-CD8 (Clone: 53-6.7)	BD Horizon	Cat# 560778; RRID: AB_1937329
anti-CD4 (Clone: RM4-4)	Invitrogen	Cat# 25-0042-82; RRID: AB_469578
anti-CD44 (Clone: IM7)	Biolegend	Cat# 103049; RRID: AB_2562600
anti-FoxP3 antibody (Clone: FJK-16S)	Invitrogen	Cat# 25-5773-82; RRID: AB_891552
anti-CD19 (Clone: 6D5)	Biolegend	Cat# 115511; RRID: AB_313646
anti-CD25 (Clone: PC61)	Biolegend	Cat# 102011; RRID: AB_312860
anti-NK1.1 (Clone: PK136) apc	Biolegend	Cat# 108709; RRID: AB_313396
anti-TCRγ/∂ (Clone: GL3) apc	Biolegend	Cat# 118115; RRID: AB_1731824
anti-TCRβ (Clone: H57-597) percp cy5.5	Biolegend	Cat# 109227; RRID: AB_1575176
anti-CD5 (Clone: 53-7.3)	Invitrogen	Cat# 11-0051-82; RRID: AB_464908
anti-cleaved caspase 3 (Asp175) (Clone:D3E9)	Cell Signaling	Cat# 12768; RRID: AB_2798021
anti-IFNγ (Clone: AN-18)	eBioscience	Cat# 14-7313-81; RRID: AB_468471
anti-IFNγ (Clone: R4-6A2)	eBioscience	Cat# 14-7312-85; RRID: AB_468470
anti-CD11b	eBioscience	Cat# 48-0112-82; RRID: AB_1582236
anti-CD11c	eBioscience	Cat# 48-0114-82; RRID: AB_1548654
anti-B220	eBioscience	Cat# 48-0452-82; RRID: AB_1548761
anti-CD8a	BD Bioscience	Cat# 560776; RRID: AB_1937317
anti-CD44	Biolegend	Cat# 103049; RRID: AB_2562600
anti-CD90.2	eBioscience	Cat# 46-0903-82; RRID: AB_10670882
anti-CD4	Biolegend	Cat# 100545; RRID: AB_11126142
Anti-CD16/32	eBioscience	Cat# 14-0161-81; RRID: AB_467132
Bacterial and virus strains		
Mouse-adapted H1N1 influenza (A/Puerto Rico/8/1934 [PR8])	Trudeau Institute	N/A
Chemicals, peptides, and recombinant proteins		
2W:I-A^b PE	Laboratory of Marc Jenkins	N/A
2W:I-A^b APC	Laboratory of Marc Jenkins	N/A
$ApoB_{p6}$:I-A^b PE	Laboratory of Marc Jenkins	N/A
$ApoB_{p6}$:I-A^b APC	Laboratory of Marc Jenkins	N/A
$NP_{366-374}/D^b$	The MBCF core facility at Trudeau Institute	N/A
$PA_{224-233}/D^b$	The MBCF core facility at Trudeau Institute	N/A

REAGENT or RESOURCE	SOURCE	IDENTIFIER
N-acetyl-L-cysteine	Sigma-Aldrich	Cat# A7250; CAS: 616-91-1
ApoB peptide (GAYSNASSTESAS)	Genescript	N/A
Desatinib	Tocris Bioscience	Cat# 6793
Critical commercial assays		
SuperScript OneCycle cDNA Kit	ThermoFisher	Cat# A10752030
BioArray High Yield RNA Transcript kit	Enzo	Cat# 50-201-2524
CellsDirect one-Step RT-PCR kit	Invitrogen	Cat# 11753-100
TRIzol	ThermoFisher	Cat# 15596026
DNAse I	NEB	Cat# M0303S
Taqman Gene Expression mix	Applied Biosystems	Cat# 4370074
Deposited data		
Raw and analyzed microarray data	This paper	GEO: GSE189279
Experimental models: Organisms/strains		
Mouse: C57BL/6J mice	The Jackson Laboratory	JAX: 000664
Mouse: mCAT Tg	The Jackson Laboratory	JAX: 016197
Oligonucleotides		
Primers for q-RT PCR, see table in methods	This paper	N/A
ApoB primer probes (20x) Mm01545156_m1	ThermoFisher	Cat# 4331182
Software and algorithms		
FlowJo software	Tree Star	https://www.flowjo.com/
GraphPad Prism	N/A	https://www.graphpad.com/scientific-software/prism/
R package version 3.0.3. and gplots	N/A	https://CRAN.R-project.org/package=gplots)